Appendix A.48:

Shirley Boys' High School – CPT 56468

Table 1: Site Description for Shirley Boys' High School (CC LIQ 35 – CPT 56468).

Attribute	Yes/No			Description/Date	Symbol in Figure 1
	10-m Buffer	20-m Buffer	50-m Buffer		
Near a body of surface water or other free face features?	No	No	No	The center of the site is ~200 m to the NW from the unnamed stream (the free-face height is ~ 3 m) and ~660 m to the NW from the Avon River (the free-face height is ~ 1.5 m).	NA
Lateral spreading observed during the CES?	No	No	No	Lateral spreading was not observed by the mapping team.[1]	NA
Nearby buildings or structures?	No	No	Yes	Building coverage of the 50-m buffer is 1%. Buildings are in the N portion of the 50-m buffer.	White Fill + Brown Outline
Sloping land?	No	No	No	Flat land, open field + residential area	NA
Step changes in the ground surface?	No	No	No	NA	NA
Retaining walls?	No	No	No	NA	NA
Vegetation?	No	No	Yes	Trees and bushes cover 12% of the 50-m buffer. They are in the N portion of the 50-m buffer.	White Fill + Green Outline
Anthropogenic changes to the site between the LiDAR surveys?	Yes	Yes	Yes	Vegetation removal from the N portion of the 50-m buffer between Jan 2006 and Mar 2009. Land resurfacing in Dec 2011 in all quadrants of all buffers. Land resurfacing in the NE, NW, and SE quadrants of all buffers in Jan 2015. Building addition in the E portion of the 50-m buffer between Sep 2015 and Nov 2015.	Building Addition: Orange Outline; Vegetation Removal: Green Crossline
Other important factors?	Yes	Yes	Yes	The sports field may be subject to re-grassing.	NA

Note: Buffer is the area within a circle of a specified radius with CPT investigations done at its center (172.659684°, -43.511008°).

[1] Canterbury Geotechnical Database. (2012). "Observed Ground Crack Locations", Map Layer CGD0400 - 23 July 2012, retrieved July 09, 2018 from https://canterburygeotechnicaldatabase.projectorbit.com/

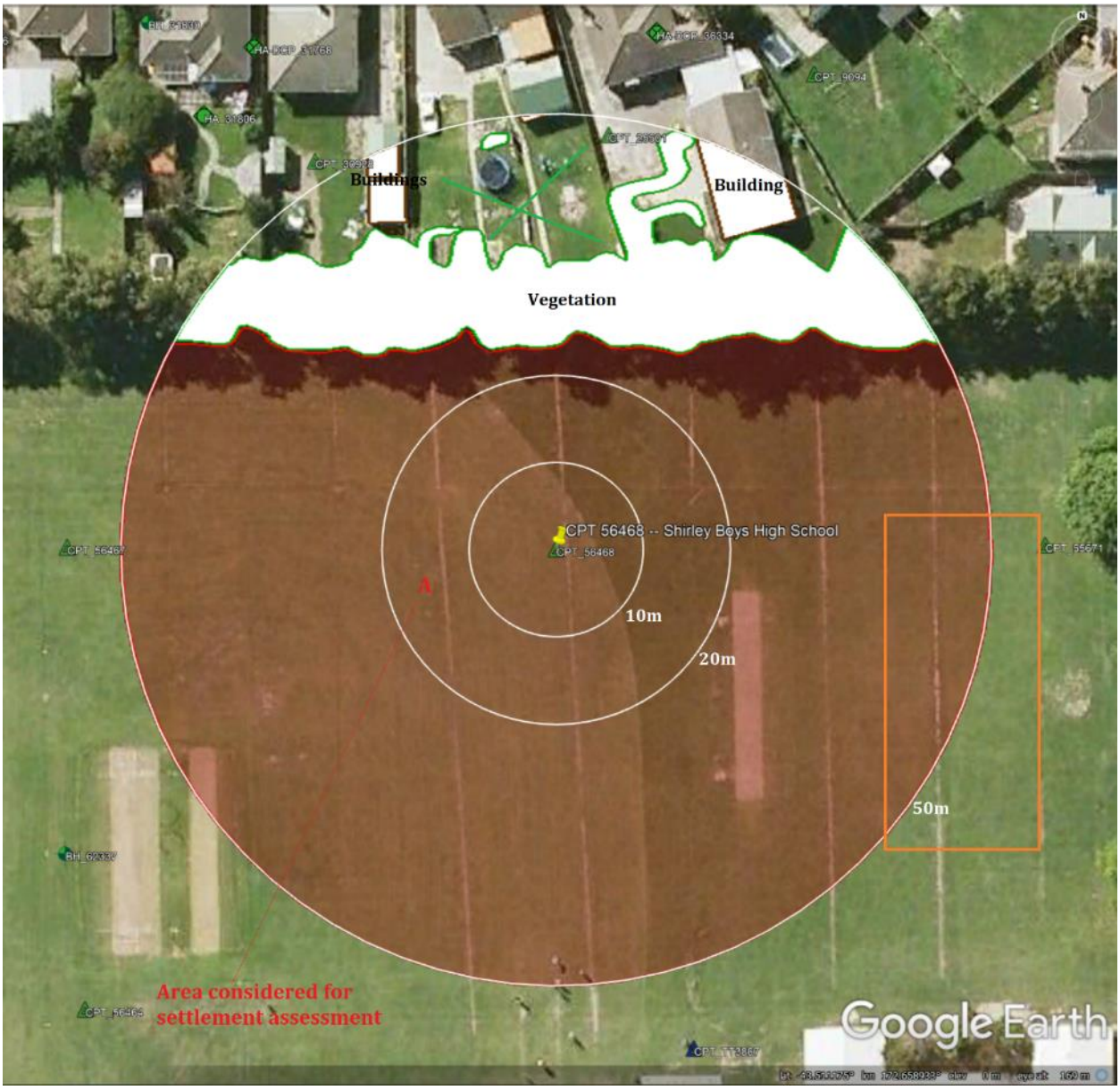

Figure 1: Site plan with areas where ejecta-induced settlement is considered.

Note 1: Patch A (outlined in red) in the free field was selected for settlement assessment as an area free of vegetation and structures. Other important factors considered in the patch selection process were its proximity to a CPT, a property subjected to addition and/or demolition of a structure, front yard/backyard alterations (e.g., ploughing, rubble, scrap), and aerial distribution of sediment ejecta. The July 2003 LiDAR survey was not used for the settlement analysis due to the evident absence of ejecta for the Sep-10 EQ. The Feb 2012 and Oct 2015 LiDAR surveys were not considered for the settlement analysis due to the anthropogenic changes.

Table 2: LiDAR flight error adjustments, global adjustments for the difference between average LiDAR point elevations and benchmark survey elevations, and vertical tectonic movement adjustments.

	Adjustments (mm)		
Earthquake Event(s)	LiDAR Flight Error	Global Offset[2]	Tectonic Vertical Movement
Sep-10	-100	-3	0
Feb-11	+100	16	-90
Jun-11	0	38	-40
Dec-11	0	-65	0
CES	0	-14	-130
Any LiDAR survey affected by ejecta?			No

Note: The negative sign indicates the subtraction from the ground surface subsidence, while the positive sign indicates the addition to the ground surface subsidence.

Table 3: LiDAR Measurement Error for Patch A.

Surveys	Buffer	Area Averaged Difference Indicating Repeat Measurement Error (mm)	$\sigma^*_{\text{individual LiDAR points}}$ (mm)	%Reduction in σ due to Area Averaging of LiDAR Points
Post Feb 2011: Mar 2011 and May 2011	10-m	45	59	[76,81]
	20-m	48		
	50-m	52		
Post Dec 2011: Feb 2012 and Oct 2015	10-m	ND	70	[ND,ND]
	20-m	ND		
	50-m	ND		

*Standard deviation; ND = Not determined due to the anthropogenic changes.

[2] Russell, J., & van Ballegooy, S. (2015). *Canterbury Earthquake Sequence: Increased liquefaction vulnerability assessment methodology*. New Zealand: Tonkin & Taylor Ltd.

Table 4: Ground surface subsidence adjustments due to LiDAR measurement error for Patch A.

Earthquake Event(s)	$\sigma_{\text{pre-EQ LiDAR survey}}$ (mm)	$\sigma_{\text{post-EQ LiDAR survey}}$ (mm)	σ_{total} (mm)	Area Average Adjusted σ (mm) **
Sep-10	158	56	134	±109
Feb-11	56	59	59	±48
Jun-11	59	61	62	±51
Dec-11	61	70	87	±70
CES	158	70	124	±101

**Based on the highest %Reduction in Table 3a.

Table 5: Raw liquefaction-related ground surface subsidence using original LiDAR points for Patch A.

	Average Ground Surface Subsidence (mm)		
Earthquake Event(s)	10-m Buffer	20-m Buffer	50-m Buffer
Sep-10	ND	ND	ND
Feb-11	182	142	99
Jun-11	59	60	54
Dec-11	ND	ND	ND
CES	ND	ND	ND

ND = Not determined.

Table 6: Corrected liquefaction-related ground surface subsidence using original LiDAR points for Patch A with the calculated adjustments in Table 2.

	Average Calculated Ground Surface Subsidence (mm)		
Earthquake Event(s)	10-m Buffer	20-m Buffer	50-m Buffer
Sep-10	ND	ND	ND
Feb-11	208±50	168±50	125±50
Jun-11	57±50	58±50	52±50
Dec-11	ND	ND	ND
CES	ND	ND	ND

Notes: Plus/minus values are same as those in Table 4a, but rounded to the nearest 25 mm; Positive overall values indicate ground surface subsidence, while negative overall values indicate ground surface uplift; ND = Not determined.

Table 7: Corrected liquefaction-related ground surface subsidence for Patch A using LiDAR DEMs.

	Estimated Ground Surface Subsidence (mm)								
	10-m Buffer			20-m Buffer			50-m Buffer		
Earthquake Event(s)	16th %ile	50th %ile	84th %ile	16th %ile	50th %ile	84th %ile	16th %ile	50th %ile	84th %ile
Sep-10	<50	<50	50	<50	<50	50	<50	<50	50
Feb-11	150	200	250	150	200	250	150	150	200
Jun-11	<50	50	50	<50	50	50	<50	50	50
Dec-11	ND	ND	ND	ND	ND	ND	ND	ND	ND
CES	ND	ND	ND	ND	ND	ND	ND	ND	ND

Note: These percentiles are not the exact statistical measures; they indicate the spatial variability of ground surface subsidence; ND = Not determined due to the anthropogenic changes.

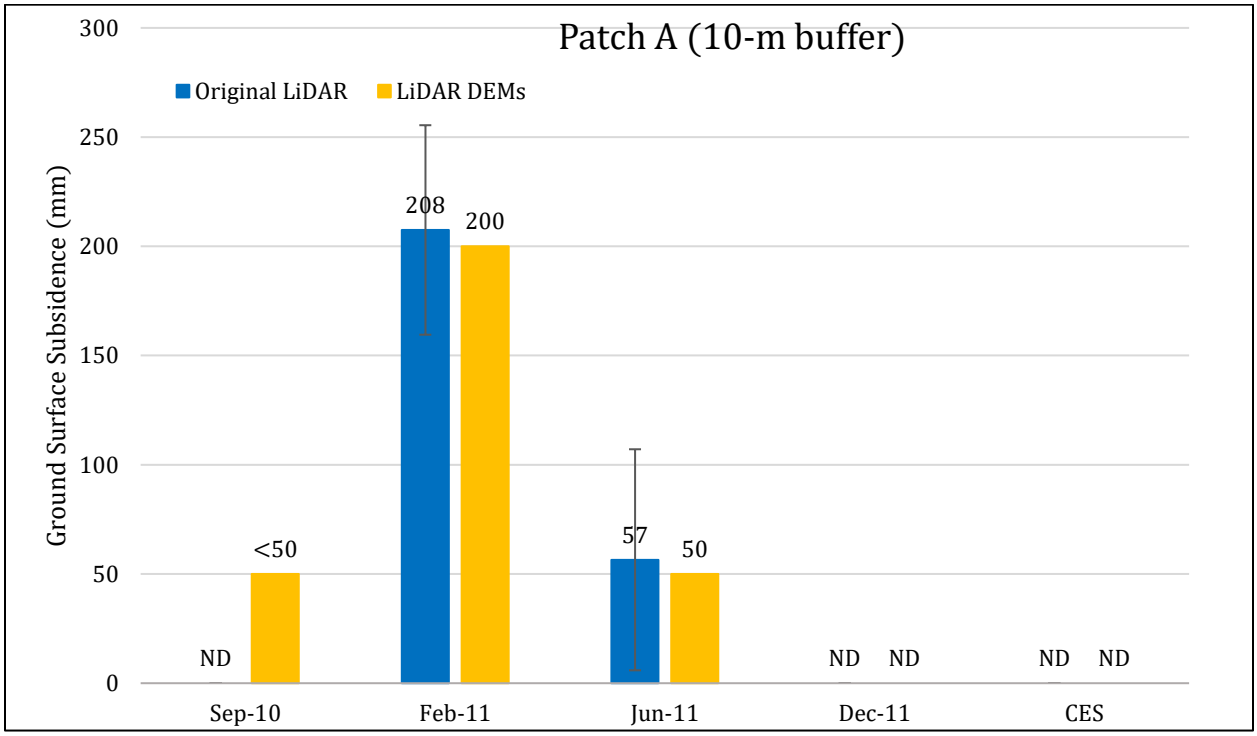

Figure 2: Comparison between ground surface subsidence determined from original LiDAR survey points and ground surface subsidence (50th %ile) estimated using LiDAR DEMs for Patch A (10-m buffer).

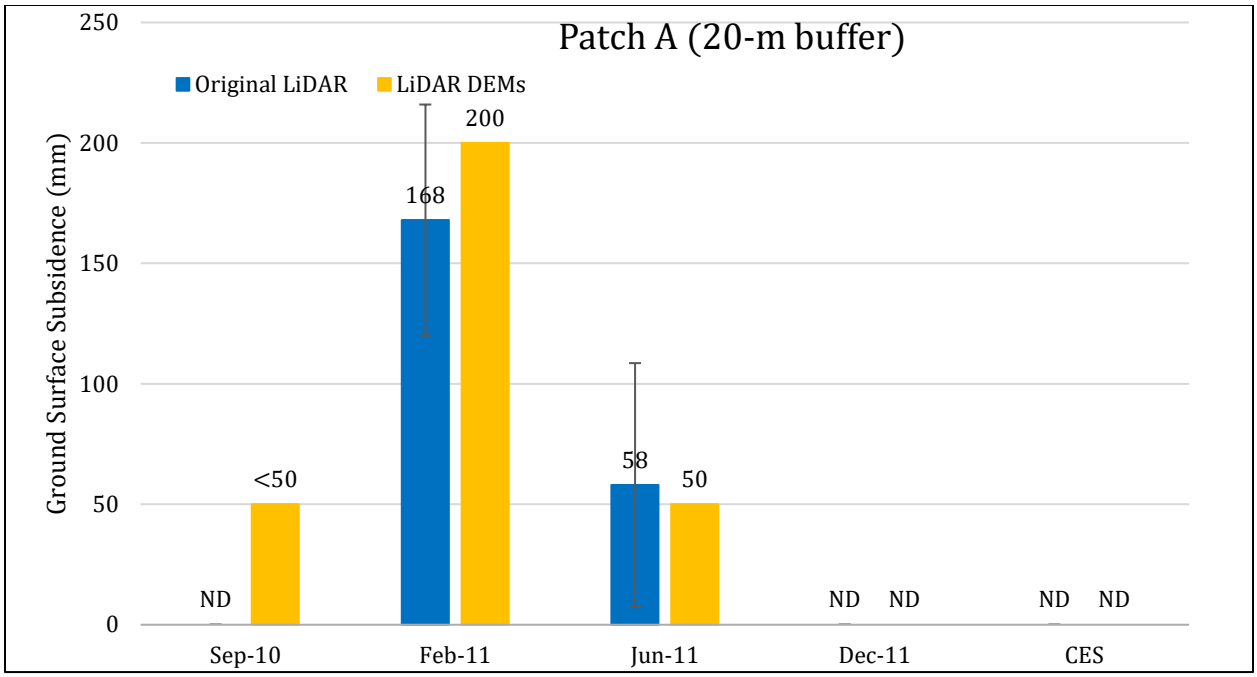

Figure 3: Comparison between ground surface subsidence determined from original LiDAR survey points and ground surface subsidence (50th %ile) estimated using LiDAR DEMs for Patch A (20-m buffer).

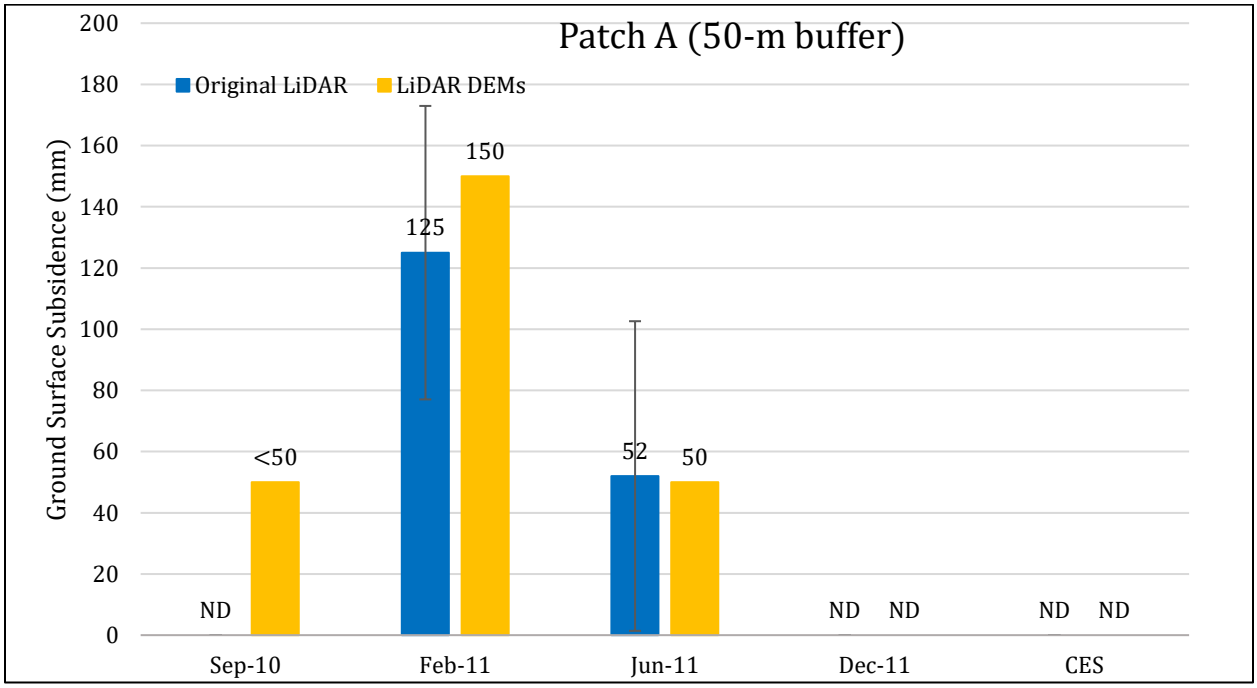

Figure 4: Comparison between ground surface subsidence determined from original LiDAR survey points and ground surface subsidence (50th %ile) estimated using LiDAR DEMs for Patch A (50-m buffer).

Note 2: The ground surface subsidence values determined from original LiDAR survey points are similar to the ground surface subsidence values estimated using LiDAR DEMs for both the Feb-11 and Jun-11 EQs. The subsidence was not estimated for the Feb-11 EQ due to the anthropogenic changes. The subsidence for the Sep-10 EQ was not determined using the original LiDAR survey points due to the evident absence of ejecta.

Table 8a: Ejecta-Induced settlement for the top 20 m of the soil profile for Patch A (10-m buffer) for the 50th %ile PGA, P_L=50%, and C_{FC}=0.13 using BI-2014, ZRB-2002, and I_c cutoff of 2.6.

Earthquake Event(s)	M_W	PGA (g)	Depth to Groundwater (m)	S_T (mm)	S_{V1D} (mm)	$S_{E,L}$ (mm)
Sep-10	7.1	0.20	1.5	ND	15±20	ND
Feb-11	6.2	0.39	1.5	208±50	83±50	125±71
Jun-11	6.2	0.22	1.5	57±50	10±25	47±56
Dec-11	6.1	0.26	1.2	ND	31±50	ND

Notes: S_T = Total settlement (Table 6); S_{V1D} = Average vertical settlement due to volumetric compression using Boulanger and Idriss (2014) (BI-2014), Zhang et al. (2002) (ZRB-2002) procedures and de Greef and Lengkeek (2018) thin-layer correction; $S_{E,L}$ = Ejecta-induced settlement as the difference between the LiDAR-based S_T and S_{V1D}; ND = Not determined.

Table 8b: Ejecta-Induced settlement for the top 20 m of the soil profile for Patch A (20-m buffer) for the 50th %ile PGA, P_L=50%, and C_{FC}=0.13 using BI-2014, ZRB-2002, and I_c cutoff of 2.6.

Earthquake Event(s)	M_W	PGA (g)	Depth to Groundwater (m)	S_T (mm)	S_{V1D} (mm)	$S_{E,L}$ (mm)
Sep-10	7.1	0.20	1.5	ND	15±20	ND
Feb-11	6.2	0.39	1.5	168±50	83±50	85±71
Jun-11	6.2	0.22	1.5	58±50	10±25	48±56
Dec-11	6.1	0.26	1.2	ND	31±50	ND

Notes: S_T = Total settlement (Table 6); S_{V1D} = Average vertical settlement due to volumetric compression using Boulanger and Idriss (2014) (BI-2014), Zhang et al. (2002) (ZRB-2002) procedures and de Greef and Lengkeek (2018) thin-layer correction; $S_{E,L}$ = Ejecta-induced settlement as the difference between the LiDAR-based S_T and S_{V1D}; ND = Not determined.

Table 8c: Ejecta-Induced settlement for the top 20 m of the soil profile for Patch A (50-m buffer) for the 50th %ile PGA, P_L=50%, and C_{FC}=0.13 using BI-2014, ZRB-2002, and I_C cutoff of 2.6.

Earthquake Event(s)	M_W	PGA (g)	Depth to Groundwater (m)	S_T (mm)	S_{V1D} (mm)	$S_{E,L}$ (mm)
Sep-10	7.1	0.20	1.5	ND	22±20	ND
Feb-11	6.2	0.39	1.5	125±50	96±50	29±71
Jun-11	6.2	0.22	1.5	52±50	14±25	38±56
Dec-11	6.1	0.26	1.2	ND	37±50	ND

Notes: S_T = Total settlement (Table 6); S_{V1D} = Average vertical settlement due to volumetric compression using Boulanger and Idriss (2014) (BI-2014), Zhang et al. (2002) (ZRB-2002) procedures and de Greef and Lengkeek (2018) thin-layer correction; $S_{E,L}$ = Ejecta-induced settlement as the difference between the LiDAR-based S_T and S_{V1D}; ND = Not determined.

Note 3: The uncertainty for volumetric settlement was derived based on the sensitivity of volumetric settlement to PGA, C_{FC}, and P_L for each earthquake event for VsVp 57203 *Shirley Intermediate School* and CC LIQ 1 – CPT 5586 – *Vivian St* sites. Taking the 50th percentile as the baseline case, the minimum and maximum values corresponding to the difference between the 25th percentile and the 50th percentile and the 75th percentile and the 50th percentile were determined. The arithmetic mean of the range of the minimum and maximum difference was evaluated for each patch at the two sites. The maximum arithmetic mean for each earthquake event was rounded to the nearest five and used as the uncertainty value. Accordingly, the 1-D volumetric settlement uncertainties of ±20, ±50, ±25, and ±50 mm for the Sep-10, Feb-11, Jun-11, and Dec-11 earthquake events, respectively, were used for all sites in this study.

Table 9a: Coverage area and height of ejecta estimates for Patch A (10-m buffer) within the 20-m buffer using photographs.

EQ Event	$A_{E,thick1}$ (m^2)	$H_{E,thick1}$ (m)	$A_{E,thick2}$ (m^2)	$H_{E,thick2}$ (m)	$A_{E,thin1}$ (m^2)	$H_{E,thin1}$ (m)	$A_{E,thin2}$ (m^2)	$H_{E,thin2}$ (m)	A_T (m^2)
Sep-10	0	0	0	0	0	0	0	0	314
Feb-11	0	0	0	0	7.2	10-20	307	5-10	314
Jun-11	0	0	61.4	60-100	3.0	20-40	218	5-10	314
Dec-11	20.4	60-120	13.6	20-40	168	10-20	1.7	2-4	314

Notes: $A_{E,thick/thin}$ = Coverage area of thick/thin ejecta layers; $H_{E,thick/thin}$ = Lower-upper estimate of height of thick/thin ejecta layers; A_T= Total assessment area of a buffer being considered.

Table 9b: Coverage area and height of ejecta estimates for Patch A (20-m buffer) using photographs.

EQ Event	$A_{E,thick1}$ (m^2)	$H_{E,thick1}$ (m)	$A_{E,thick2}$ (m^2)	$H_{E,thick2}$ (m)	$A_{E,thin1}$ (m^2)	$H_{E,thin1}$ (m)	$A_{E,thin2}$ (m^2)	$H_{E,thin2}$ (m)	A_T (m^2)
Sep-10	0	0	0	0	0	0	0	0	1257
Feb-11	68.6	100-150	0	0	280	10-20	908	5-10	1257
Jun-11	0	0	164	60-100	27.4	20-40	717	5-10	1257
Dec-11	58.9	60-120	24.4	20-40	583	10-20	106	2-4	1257

Notes: $A_{E,thick/thin}$ = Coverage area of thick/thin ejecta layers; $H_{E,thick/thin}$ = Lower-upper estimate of height of thick/thin ejecta layers; A_T= Total assessment area of a buffer being considered.

Table 9c: Coverage area and height of ejecta estimates for Patch A (50-m buffer) using photographs.

EQ Event	$A_{E,thick1}$ (m^2)	$H_{E,thick1}$ (m)	$A_{E,thick2}$ (m^2)	$H_{E,thick2}$ (m)	$A_{E,thin1}$ (m^2)	$H_{E,thin1}$ (m)	$A_{E,thin2}$ (m^2)	$H_{E,thin2}$ (m)	A_T (m^2)
Sep-10	0	0	0	0	0	0	0	0	6170
Feb-11	130	100-150	552	50-80	1662	10-20	3290	5-10	6170
Jun-11	0	0	754	60-100	79.3	20-40	2974	5-10	6170
Dec-11	122	60-120	163	20-40	1852	10-20	637	2-4	6170

Notes: $A_{E,thick/thin}$ = Coverage area of thick/thin ejecta layers; $H_{E,thick/thin}$ = Lower-upper estimate of height of thick/thin ejecta layers; A_T= Total assessment area of a buffer being considered.

Note 4: The values in Table 9 correspond to the coverage area of ejecta outlined in aerial photographs (Figures 21, 24, and 57-59) and the lower and upper estimates of ejecta height based on geometrical approximations, ground photographs (Figure 62), and EQC LDAT property inspection reports (e.g., Figures 60 and 61). The ejecta-induced settlement using photographs and engineering judgment, $S_{E,P}$, is estimated as

$$S_{E,P} = \frac{\sum_{i=1}^{a} A_{E,thick,i} * H_{E,thick,i} + \sum_{j=1}^{b} A_{E,thin,j} * H_{E,thin,j}}{A_T} = \frac{\sum_{i=1}^{a} V_{E,thick,i} + \sum_{j=1}^{b} V_{E,thin,j}}{A_T}$$

where

- $A_{E,thick,i}$ and $H_{E,thick,i}$ are the area and the height of a thick ejecta layer, respectively;
- $A_{E,thin,j}$ and $H_{E,thin,j}$ are the area and the height of a thin ejecta layer, respectively;
- A_T is the total assessment area for a buffer being considered (Figure 1).

Table 10: Ejecta-induced settlement estimates for Patch A based on photographs.

Earthquake Event	Patch A (10-m buffer)		Patch A (20-m buffer)		Patch A (50-m buffer)	
	$S_{E,P,lower}$ (mm)	$S_{E,P,upper}$ (mm)	$S_{E,P,lower}$ (mm)	$S_{E,P,upper}$ (mm)	$S_{E,P,lower}$ (mm)	$S_{E,P,upper}$ (mm)
Sep-10	0	0	0	0	0	0
Feb-11	5	10	11	20	12	21
Jun-11	15	27	11	20	10	18
Dec-11	10	20	8	16	5	10

Note: $S_{E,P,lower}$ and $S_{E,P,upper}$ correspond to lower and upper estimates of $S_{E,P}$, respectively.

Table 11: Best final estimates of ejecta-induced settlement for Patch A.

EQ Event	Patch A (10-m buffer)			Patch A (20-m buffer)			Patch A (50-m buffer)		
	$S_{E,L}$ (mm)	$S_{E,P}$ (mm)	$S_{E,final}$ (mm)	$S_{E,L}$ (mm)	$S_{E,P}$ (mm)	$S_{E,final}$ (mm)	$S_{E,L}$ (mm)	$S_{E,P}$ (mm)	$S_{E,final}$ (mm)
Sep-10	ND	0	0	ND	0	0	ND	0	0
Feb-11	125±71	8±2	10±5	85±71	16±4	25±10	29±71	17±4	20±10
Jun-11	47±56	21±6	30±20	48±56	16±4	25±20	38±56	14±4	20±20
Dec-11	ND	15±5	15±5	ND	12±4	10±5	ND	8±2	10±5

Notes: $S_{E,L}$ = Ejecta-induced settlement based on LiDAR data reported in Table 8; $S_{E,P}$ = Median ejecta-induced settlement for the range of values reported in Table 10; $S_{E,final}$ = Best final estimate of ejecta-induced settlement rounded to the nearest 5 mm; Final plus/minus values are also rounded to the nearest 5 mm; ND = Not determined.

Note 5:

- Patch A (10-m buffer): $S_{E,final}$ for the Sep-10 and Dec-11 EQs is based solely on $S_{E,P}$ due to the evident absence of ejecta for the Sep-10 EQ and the anthropogenic changes that affected the LiDAR survey measurements for the Dec-11 EQ (i.e., the Feb 2012 and Oct 2015 LiDAR surveys). $S_{E,final}$ for the Feb-11 EQ is also based on $S_{E,P}$ only due to the discrepancy between visual evidence and LiDAR-based estimates (the small quantum of ejecta versus the large quantum of ejecta, respectively). $S_{E,final}$ for the Jun-11 EQ is the weighted average of $S_{E,L}$ and $S_{E,P}$ with weights of 1/3 and 2/3, respectively. The uncertainty associated with $S_{E,final}$ is also the weighted average of uncertainties associated with $S_{E,L}$ and $S_{E,P}$ with the same respective weights of 1/3 and 2/3.
- Patch A (20-m and 50-m buffers): $S_{E,final}$ for the Sep-10 and Dec-11 EQs is based solely on $S_{E,P}$ due to the evident absence of ejecta for the Sep-10 EQ and the anthropogenic changes that affected the LiDAR survey measurements for the Dec-11 EQ (i.e., the Feb 2012 and Oct 2015 LiDAR surveys). $S_{E,final}$ for the Feb-11 EQ is a weighted average of $S_{E,L}$ and $S_{E,P}$ with weights of 0.1 and 0.9, respectively. $S_{E,final}$ for the Jun-11 EQ is the weighted average of $S_{E,L}$ and $S_{E,P}$ with weights of 1/3 and 2/3, respectively. The uncertainty associated with $S_{E,final}$ is also the weighted average of uncertainties associated with $S_{E,L}$ and $S_{E,P}$ with the same respective weights of 0.1 and 0.9 for the Feb-11 EQ and 1/3 and 2/3 for the Jun-11 EQ.

- The weight coefficients are based on the LiDAR error bands, LPI prediction error (Maurer et al. 2014[3]), presence of ejecta at the time of LiDAR surveys, discrepancy between visual evidence and LiDAR-based estimates (i.e., $S_{E,L}$ suggests more ejecta within the 10-m buffer than the 20-m and 50-m buffers even though the least quantum of ejecta is observed in the aerial photograph for the 10-m buffer), and completeness of visual evidence (i.e., ground and aerial photographs and EQC LDAT property inspection reports for the site). The Shirley Boys' High School site is in the apparent zone of higher ground surface subsidence for the Sep-10 EQ and the apparent zone of lower ground surface subsidence for the Feb-11 EQ (i.e., the overestimate of ground surface elevation by the Sep-10 LiDAR survey). The site is also in the zone of accurate LPI prediction of liquefaction severity for the Sep-10 EQ and slight to moderate LPI underprediction of liquefaction severity for the Sep-10 and Feb-11 EQ. The LDAT inspection reports and ground photographs from May 2011 are available for the properties in the N portion of the 50-m buffer (outside Patch A). The ejecta height ranged from 30 mm to 300 mm.

Summary 1:

The best estimate of the ejecta-induced free-field ground settlement at the Shirley Boys' High School site for the SEP 2010, FEB 2011, JUN 2011, and DEC 2011 earthquake is 0 mm, 25±10 mm, 25±20, and 10±5 mm, respectively.

[3] Maurer, B. W., Green, R. A., Cubrinovski, M., & Bradley, B. A. (2014). Evaluation of the Liquefaction Potential Index for Assessing Liquefaction Hazard in Christchurch, New Zealand. *Journal of Geotechnical and Geoenvironmental Engineering*, 140(7), 04014032-1-11. doi:10.1061/(asce)gt.1943-5606.0001117

Figure 5: Location of the site.

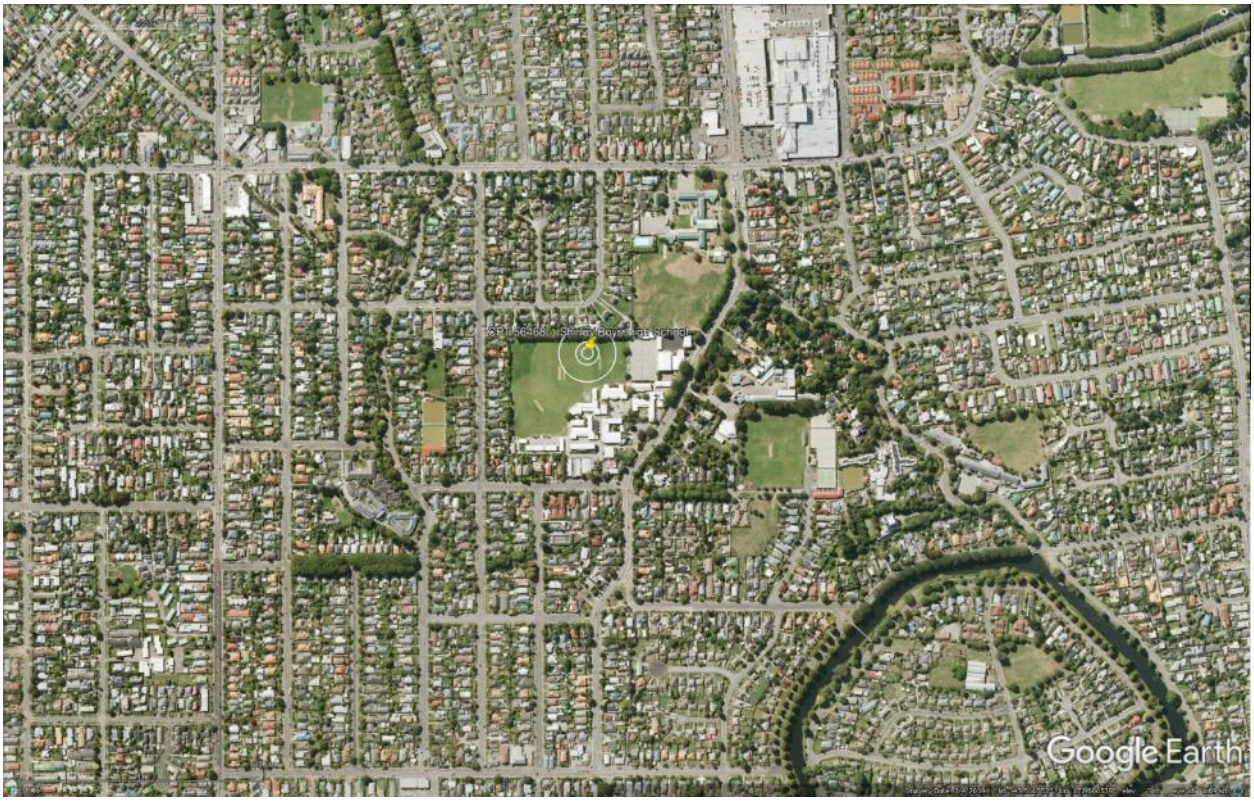

Figure 6: Position of the site relative to nearby buildings, vegetation, and free-face features.

Figure 7: Street view of the flat land.

Figure 8: Satellite image of the site taken in Dec 2004.

Figure 9: Satellite image of the site taken in Jan 2006.

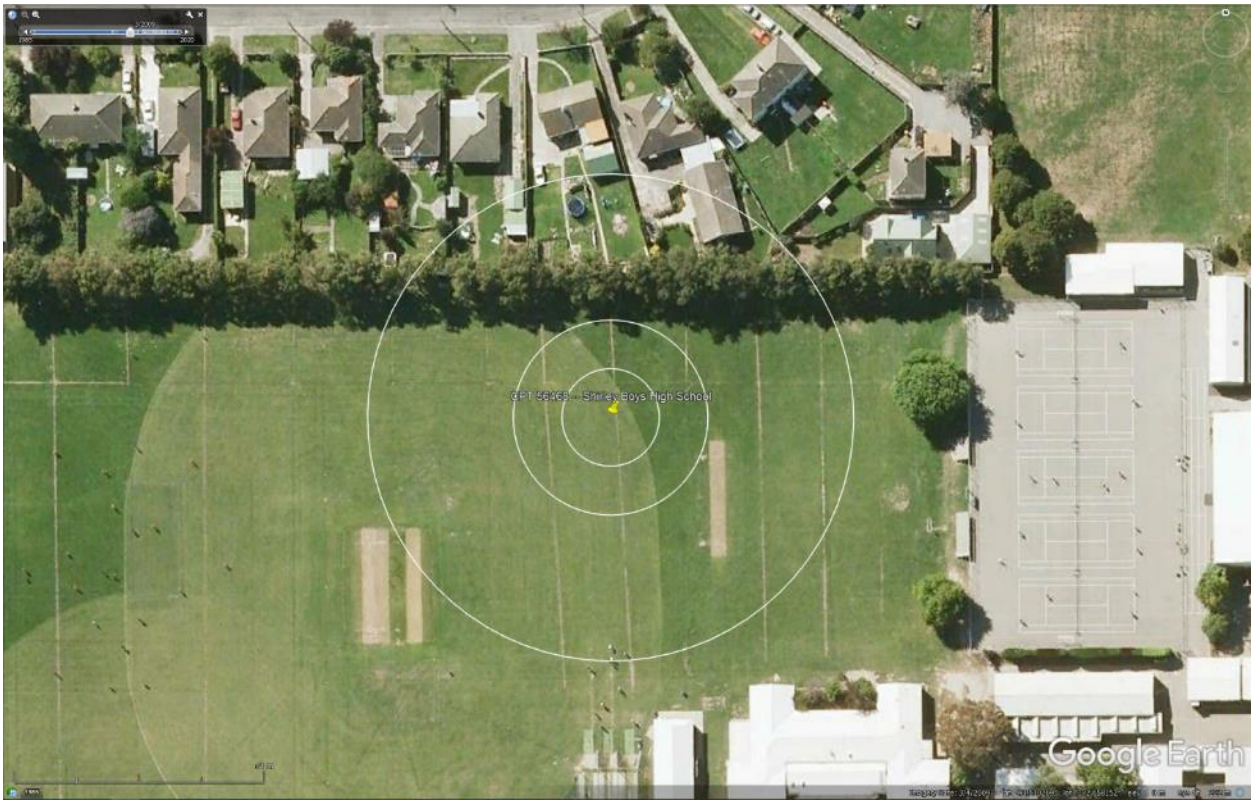

Figure 10: Satellite image of the site taken in Mar 2009.

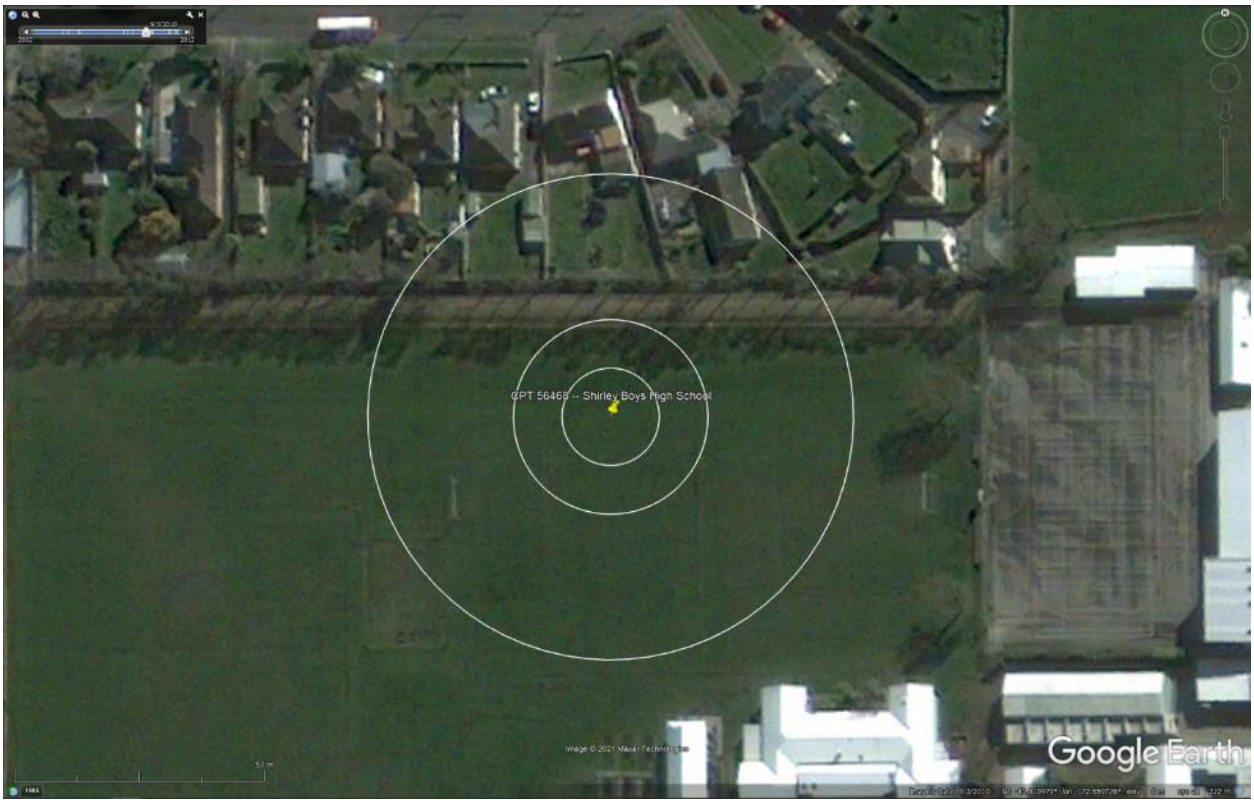

Figure 11: Satellite image of the site taken on Sep 3, 2010.

Figure 12: Satellite image of the site taken on Sep 5, 2010.

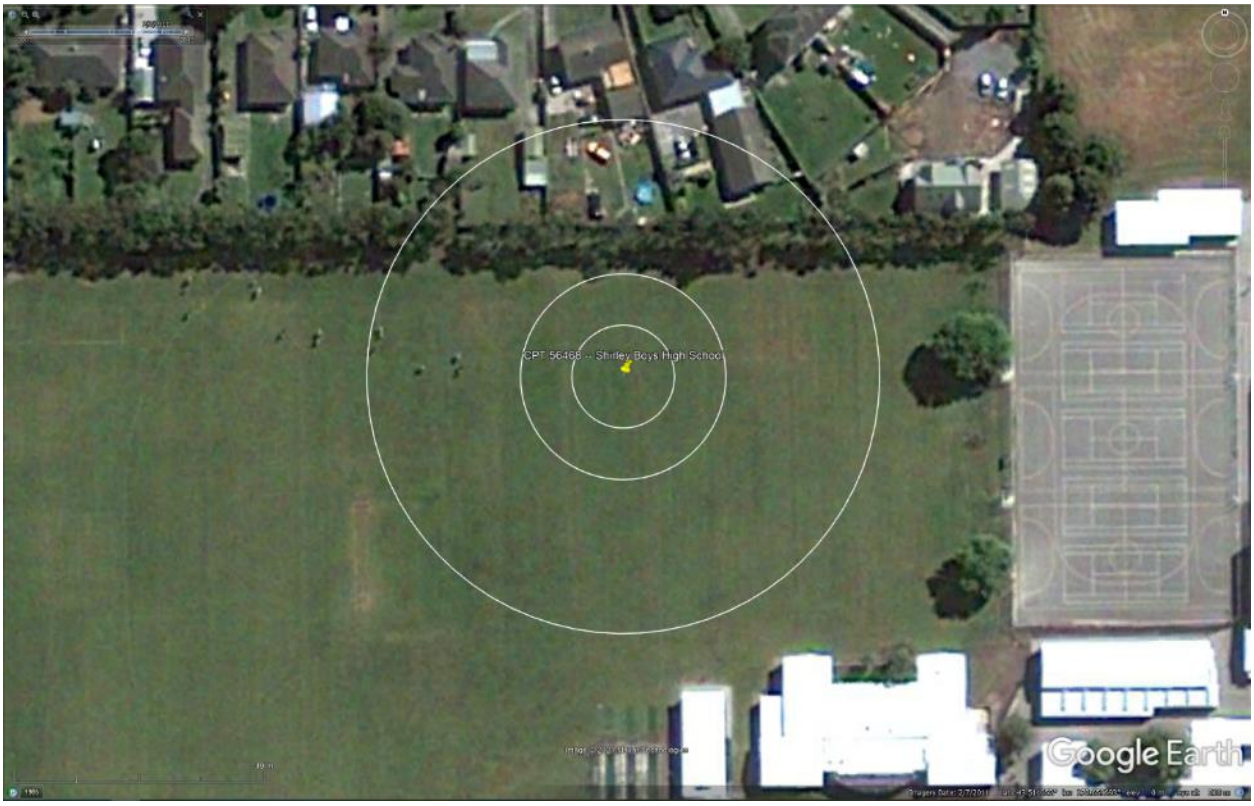

Figure 13: Satellite image of the site taken on Feb 7, 2011.

Figure 14: Satellite image of the site taken on Feb 23, 2011.

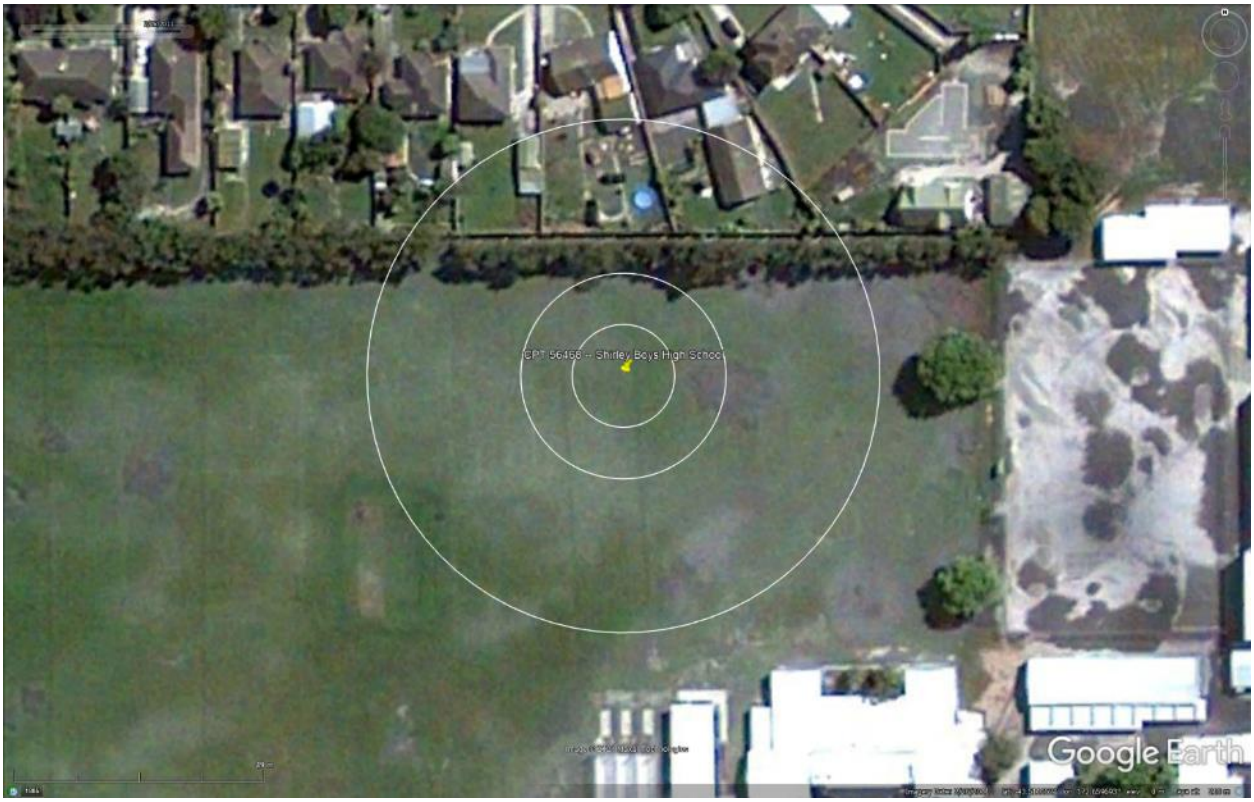

Figure 15: Satellite image of the site taken on Feb 26, 2011.

Figure 16: Satellite image of the site taken on Mar 28, 2011.

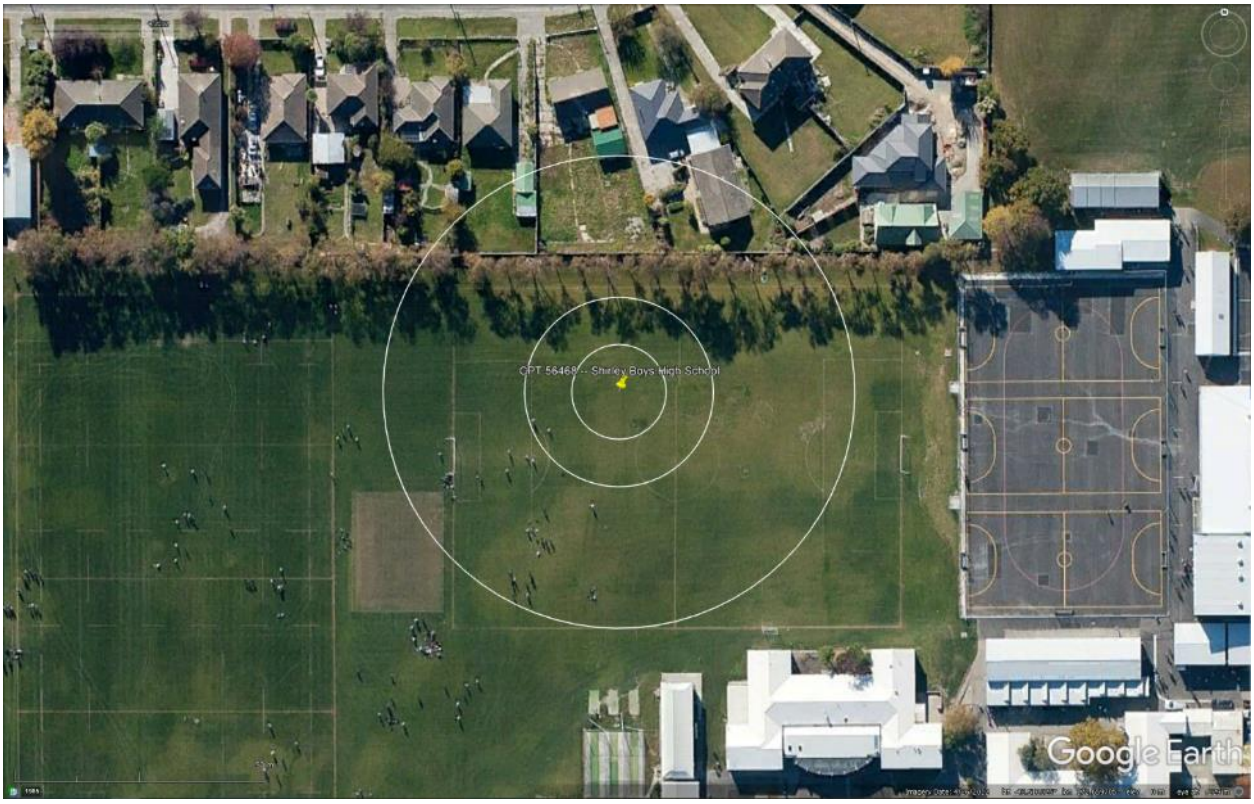

Figure 17: Satellite image of the site taken in Apr 2012.

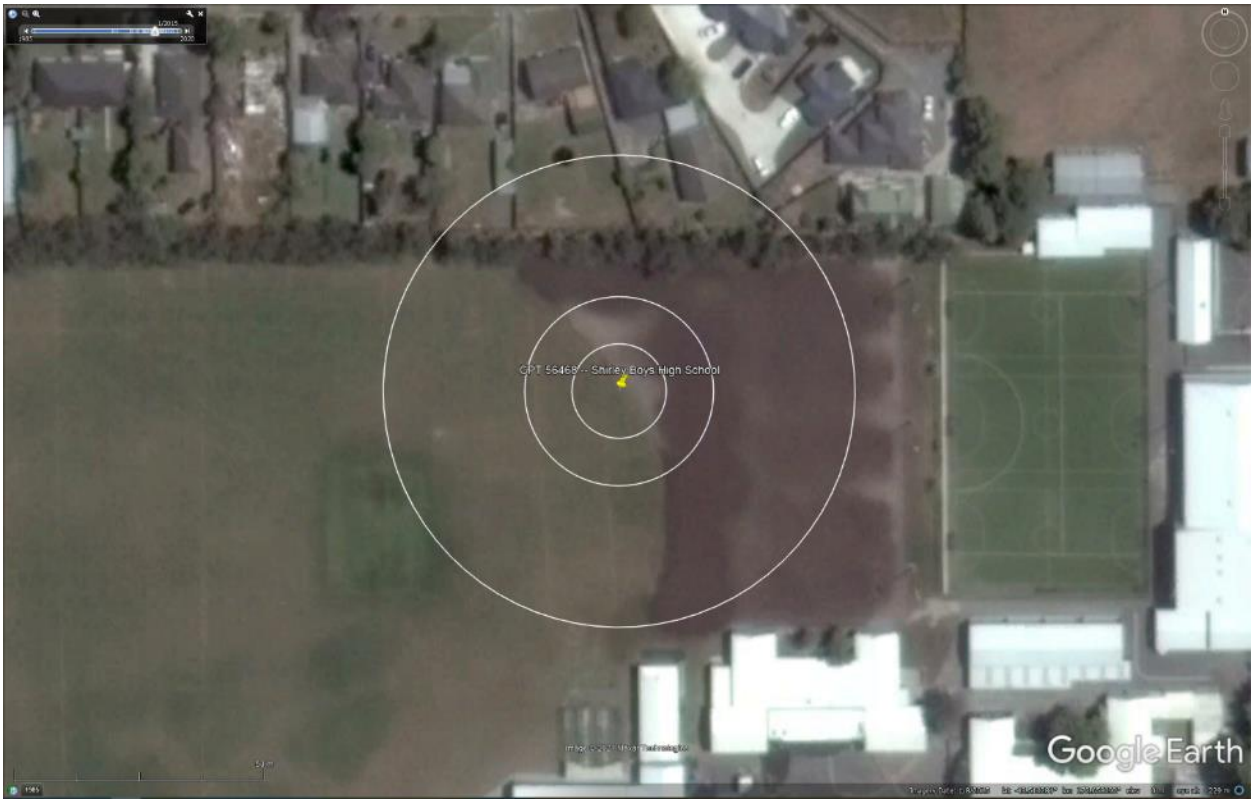

Figure 18: Satellite image of the site taken in Jan 2015.

Figure 19: Satellite image of the site taken in Sep 2015.

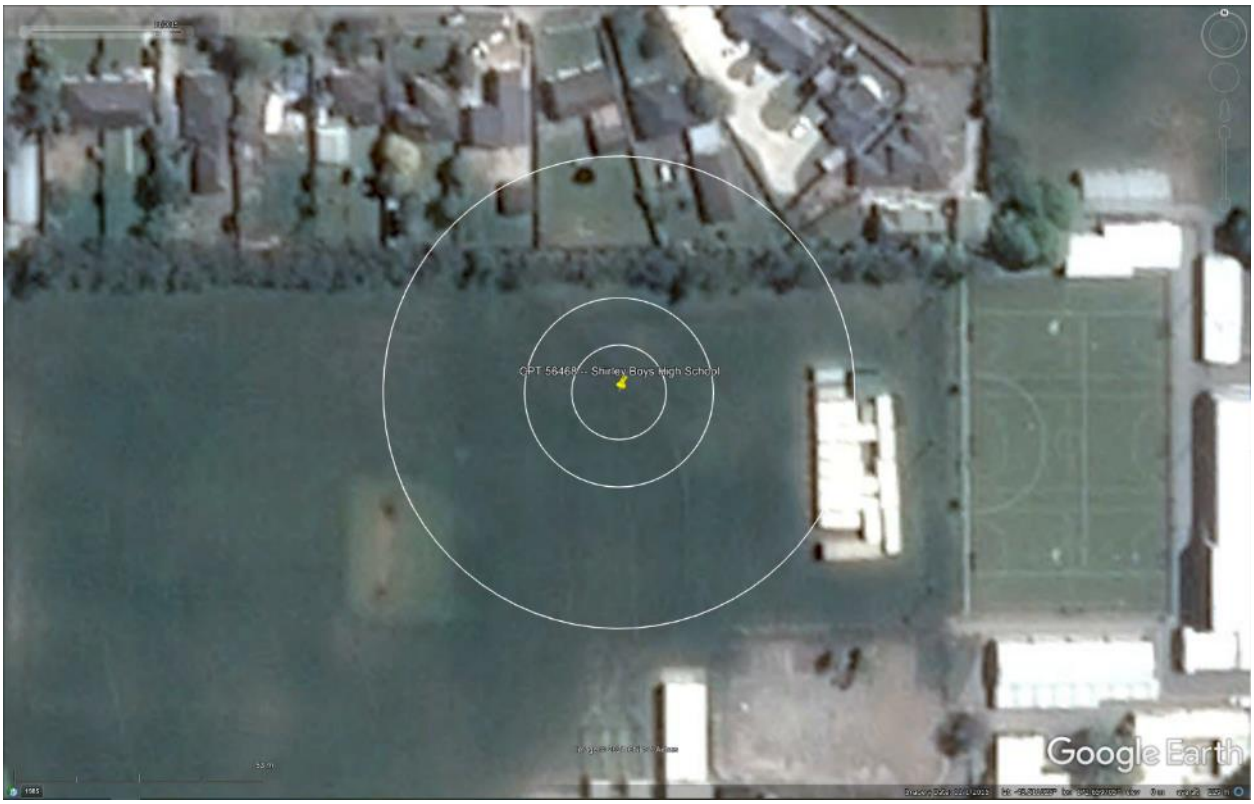

Figure 20: Satellite image of the site taken in Nov 2015.

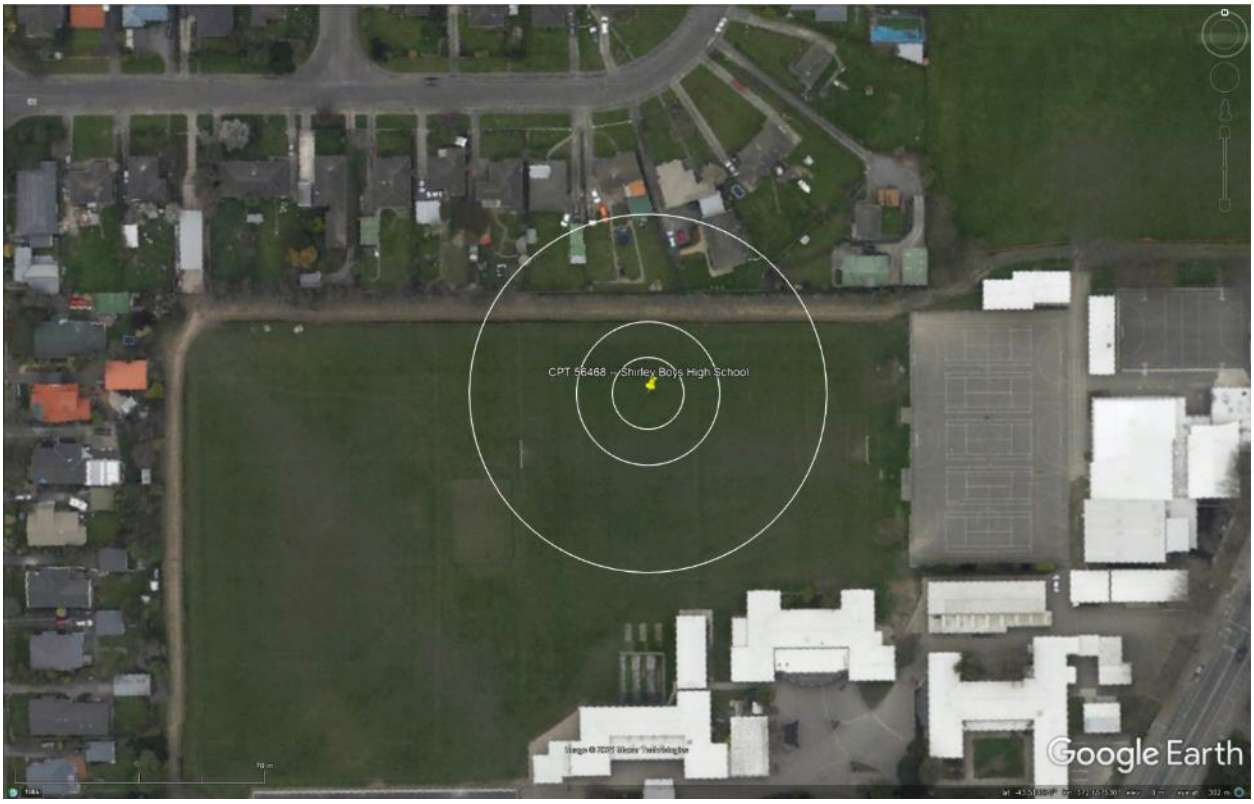

Figure 21: Aerial photograph of the site taken on Sep 4, 2010.

Figure 22: Aerial photograph of the site taken on Feb 24, 2011.

Figure 23: Aerial photograph of the site taken on June 14-15, 2011.

Figure 24: Aerial photograph of the site taken on June 16, 2011.

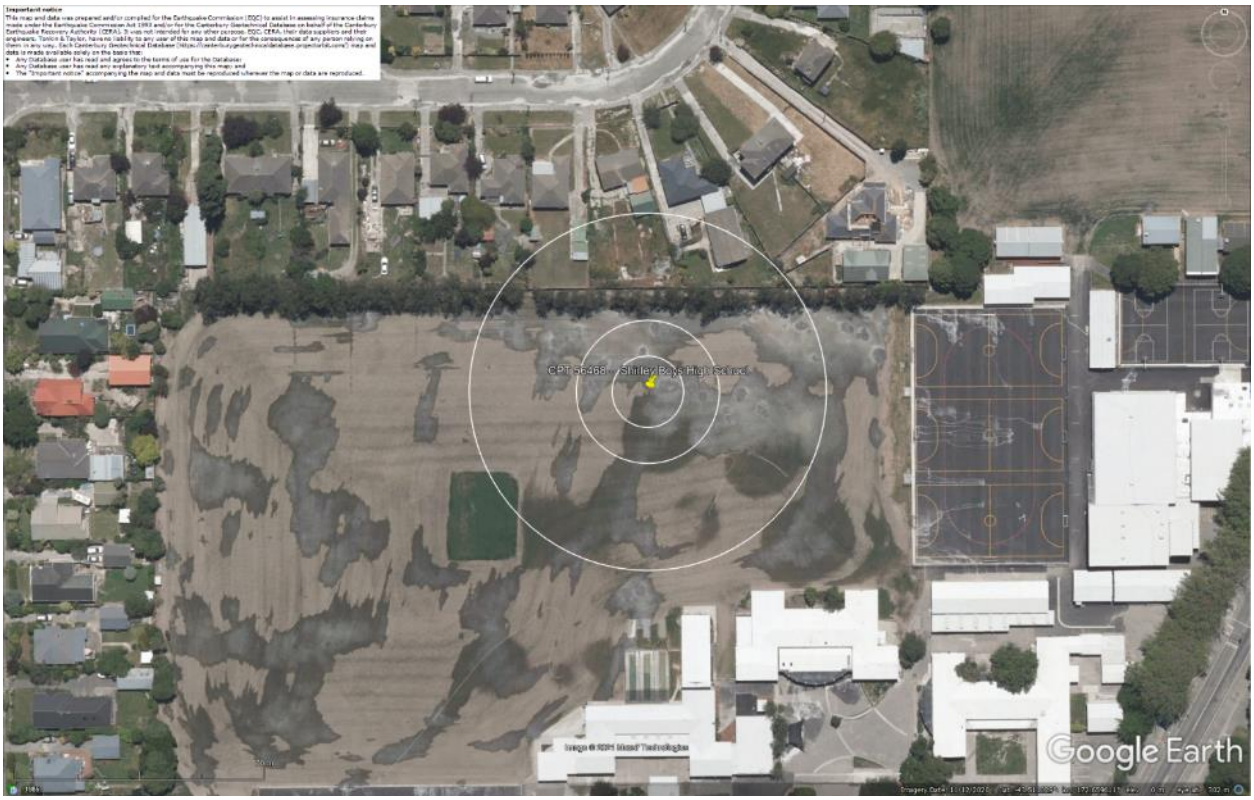

Figure 25: Aerial photograph of the site taken on Dec 24, 2011.

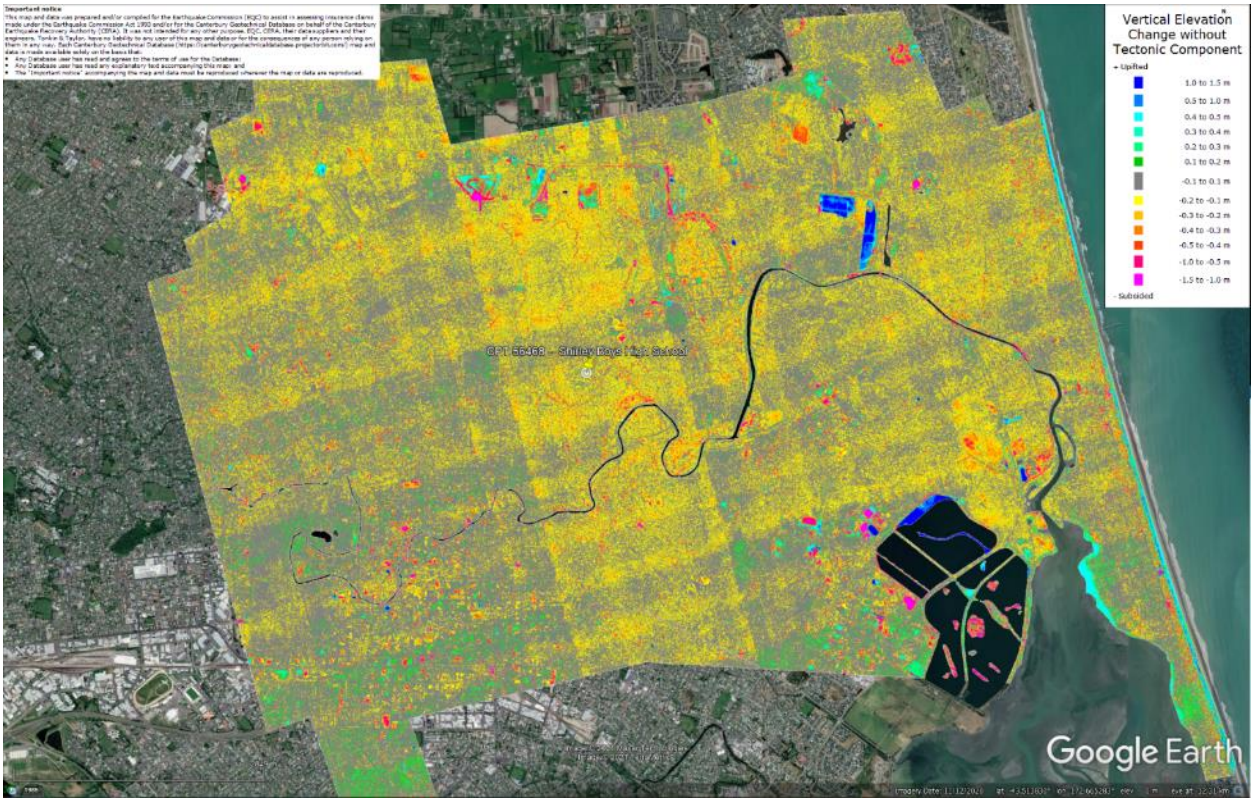

Figure 26: Vertical Ground Movements (Surface – Tectonic) for Sep 2010 Earthquake – the site is in the apparent zone of overestimated ground surface subsidence (i.e., Sep 2010 LiDAR flight error zone).

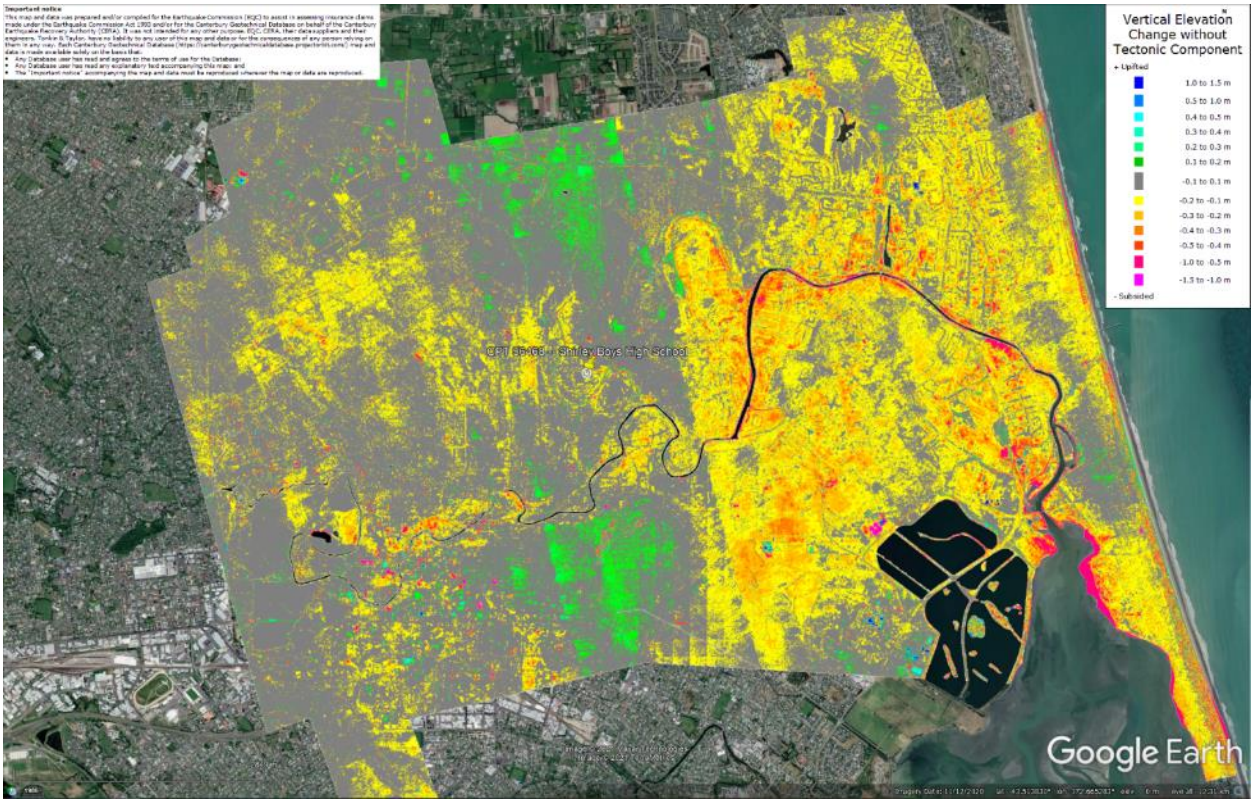

Figure 27: Vertical Ground Movements (Surface – Tectonic) for Feb 2011 Earthquake – the site is in the apparent zone of underestimated ground surface subsidence (i.e., Sep 2010 LiDAR flight error zone).

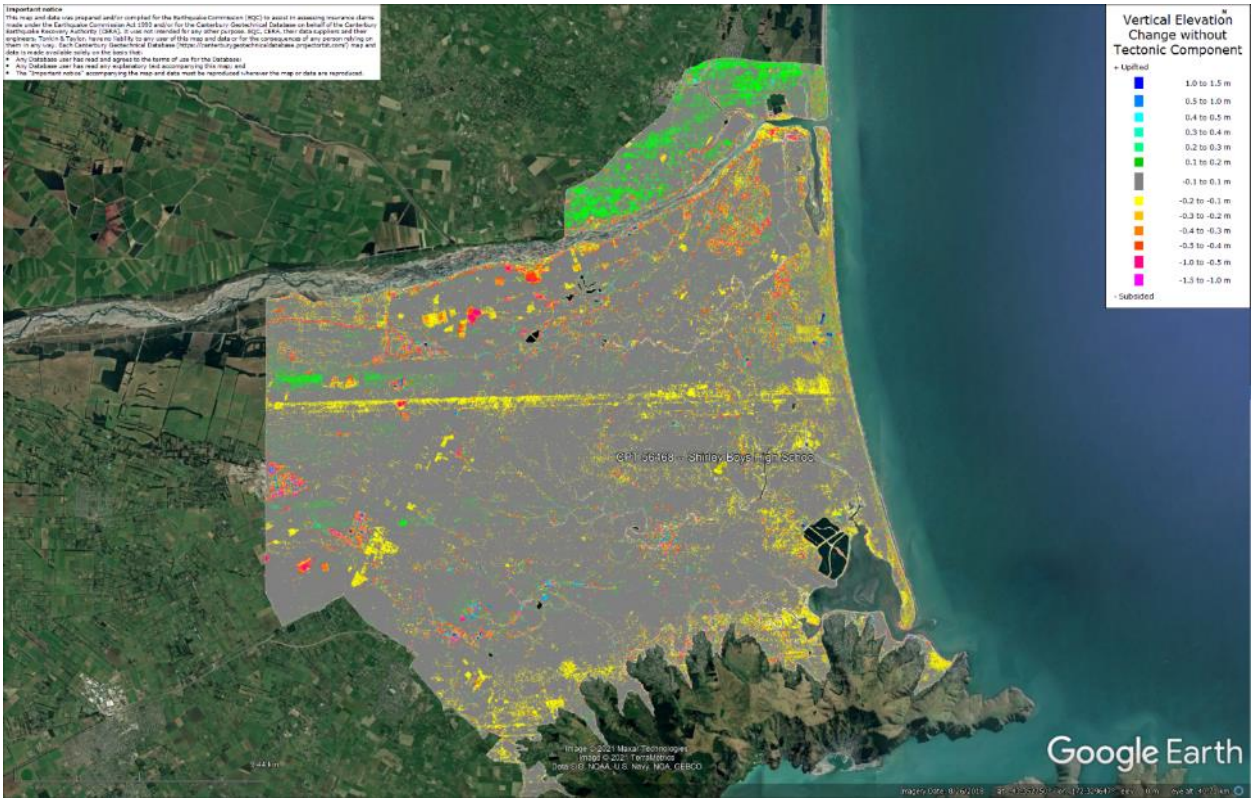

Figure 28: Vertical Ground Movements (Surface – Tectonic) for June 2011 Earthquake – the site is not in the apparent zone of overestimated ground surface subsidence.

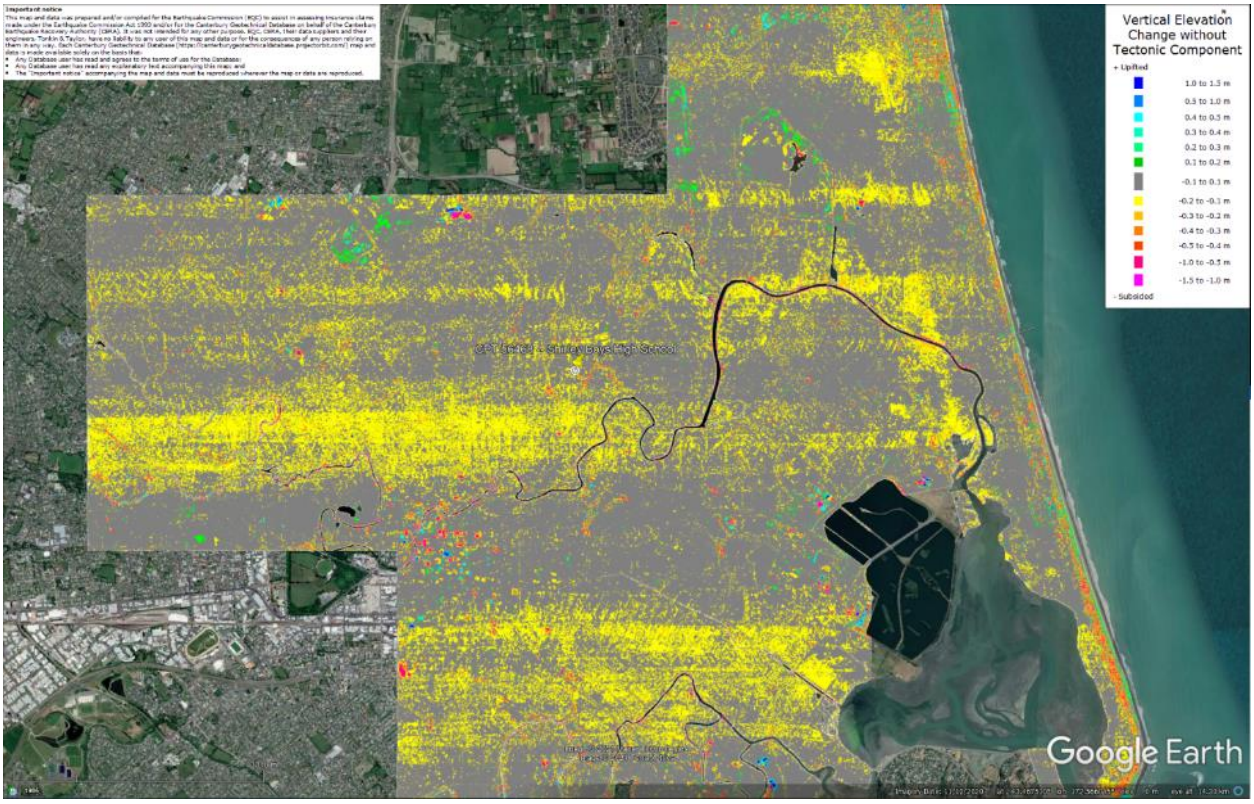

Figure 29: Vertical Ground Movements (Surface – Tectonic) for Dec 2011 Earthquake – the site is not in the apparent zone of overestimated/underestimated ground surface subsidence.

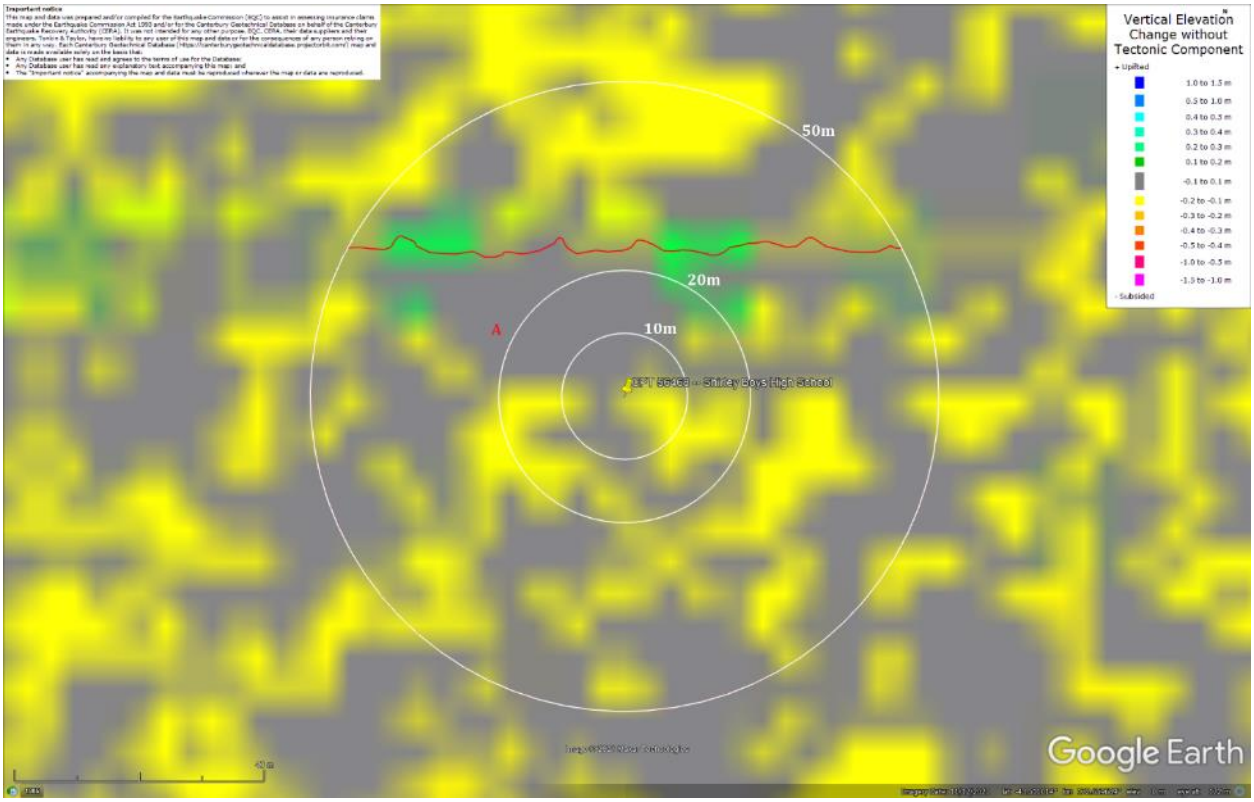

Figure 30: Ground surface subsidence without tectonic component for Sep 2010 Earthquake according to the LiDAR DEM.

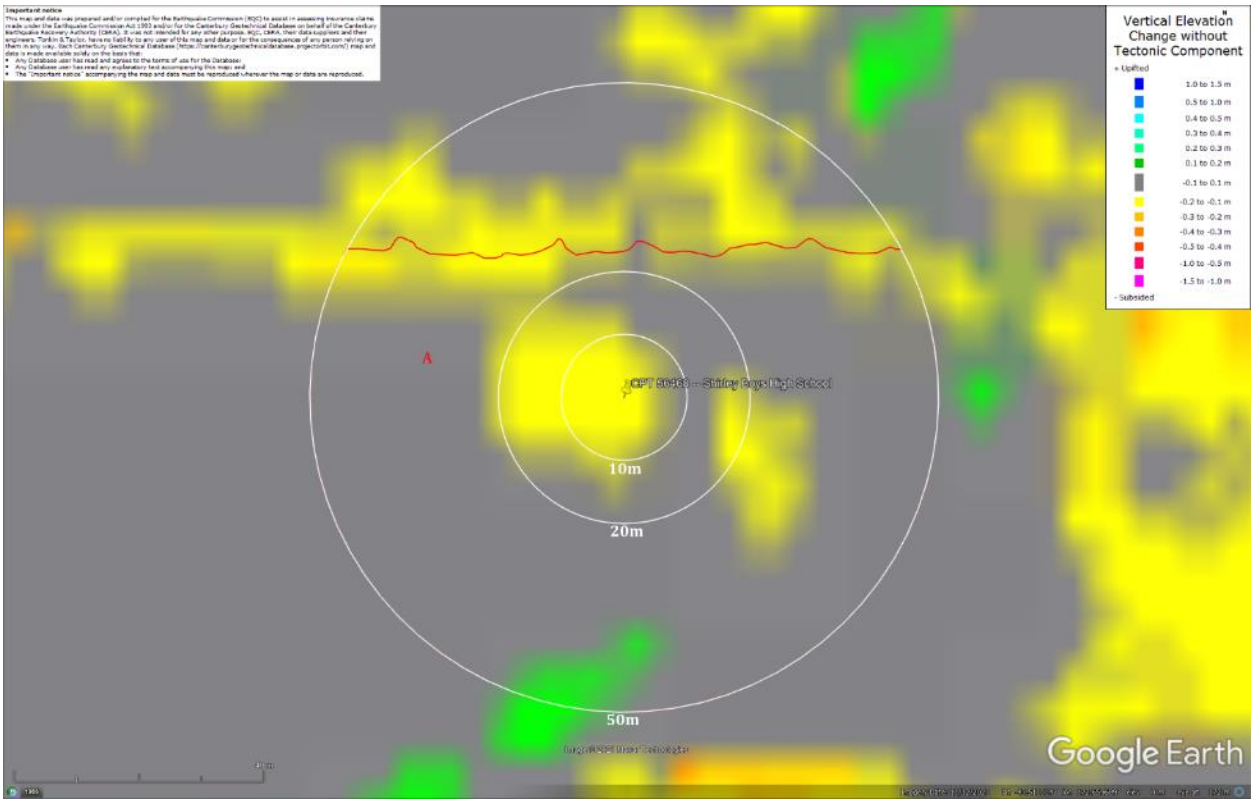

Figure 31: Ground surface subsidence without tectonic component for Feb 2011 Earthquake according to the LiDAR DEM.

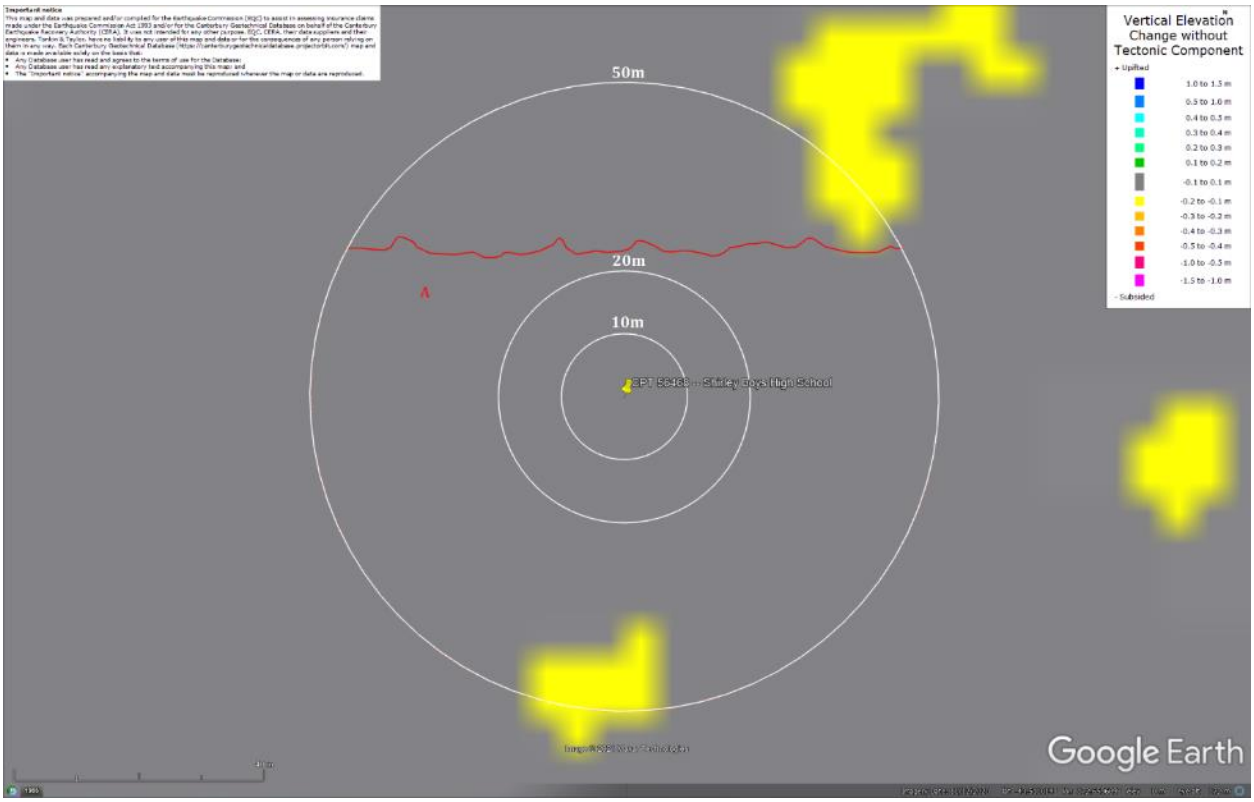

Figure 32: Ground surface subsidence without tectonic component for June 2011 Earthquake according to the LiDAR DEM.

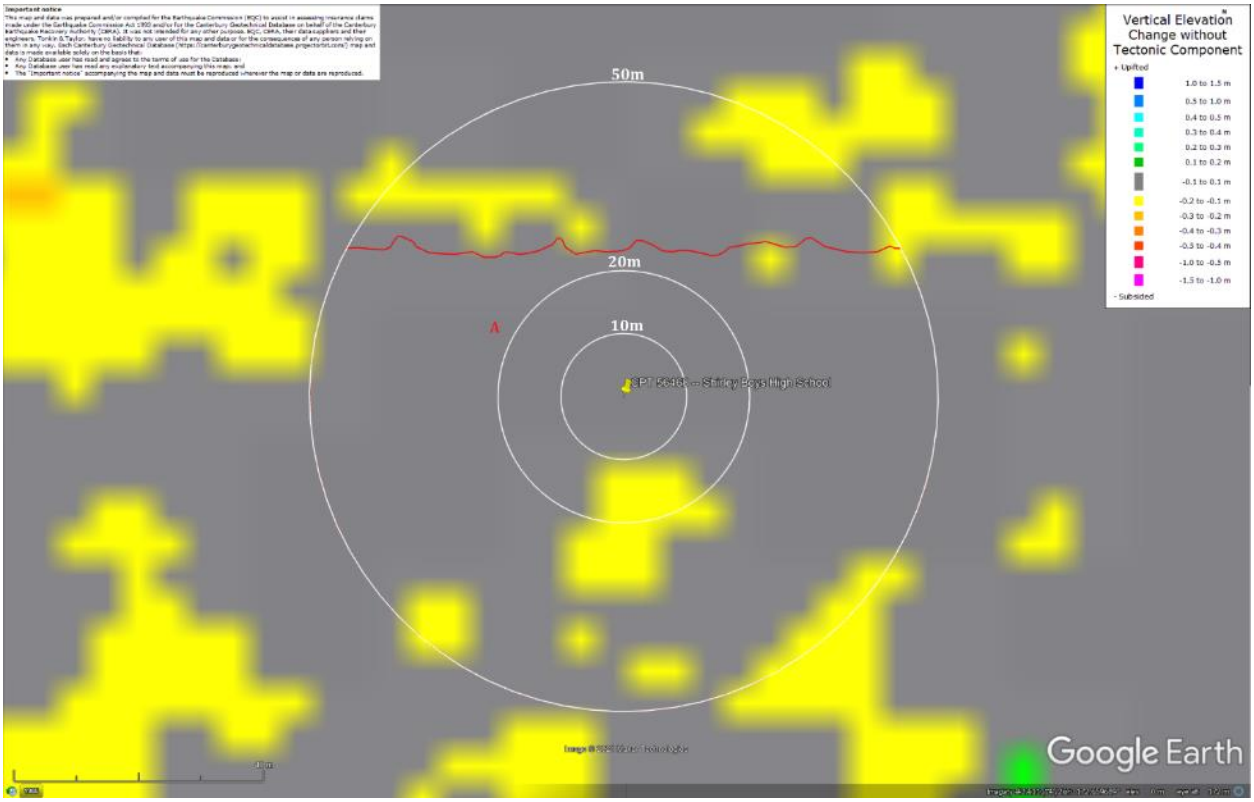

Figure 33: Ground surface subsidence without tectonic component for Dec 2011 Earthquake according to the LiDAR DEM.

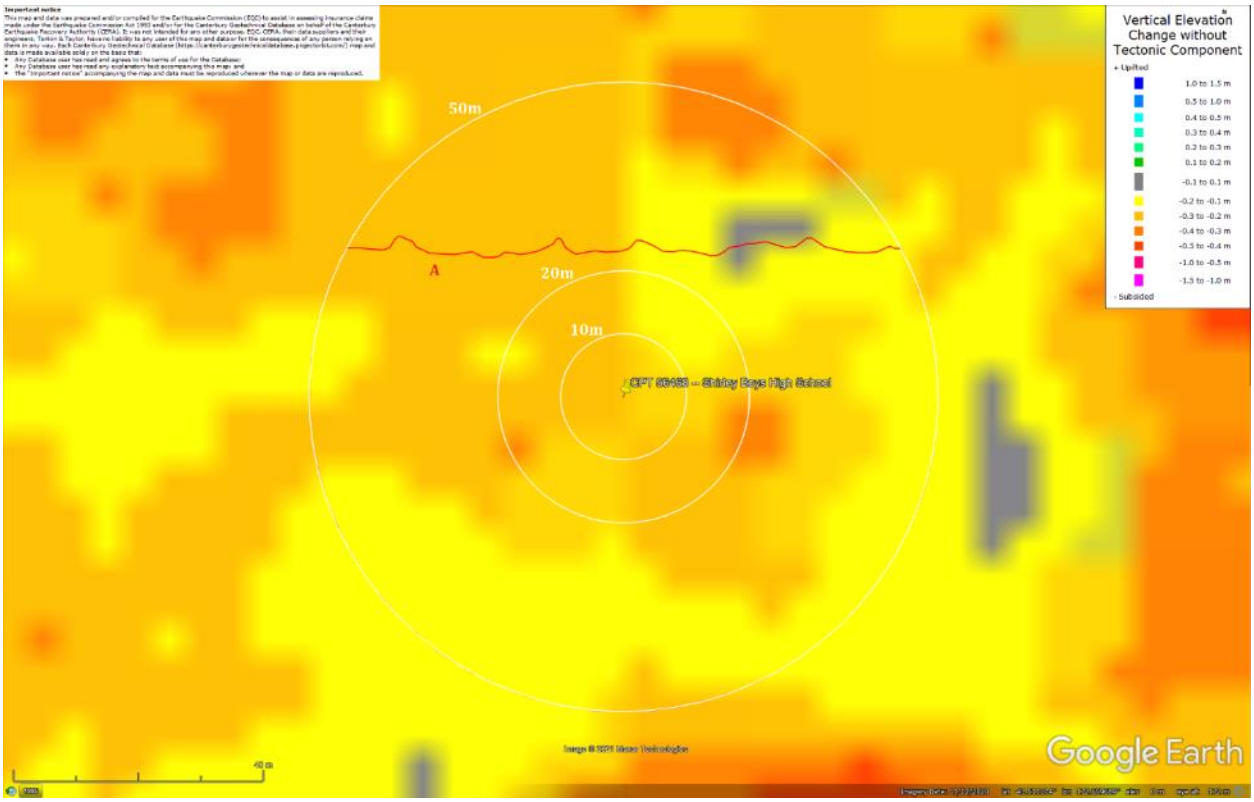

Figure 34: Ground surface subsidence without tectonic component for Canterbury Earthquake Sequence according to the LiDAR DEM.

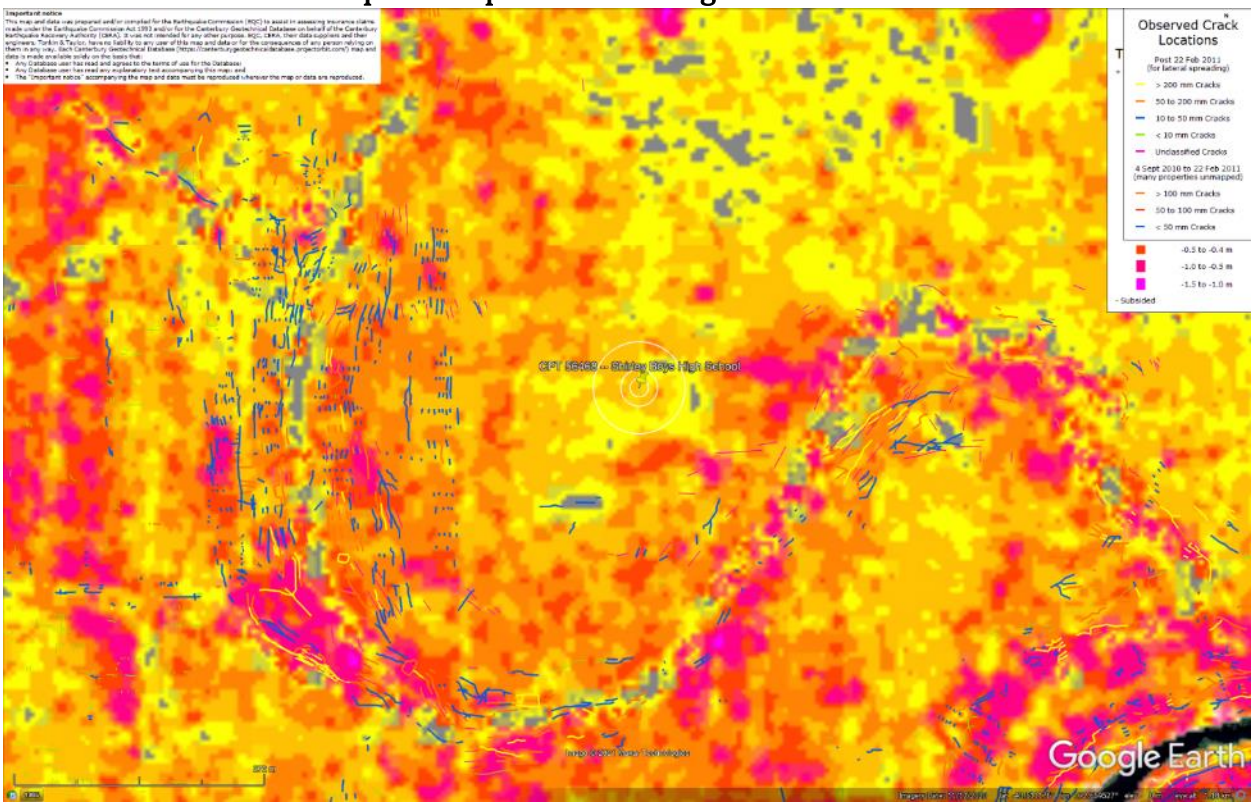

Figure 35: No lateral spreading for Canterbury Earthquake Sequence.

Figure 36: Vertical tectonic movements for Sep 2010 Earthquake.

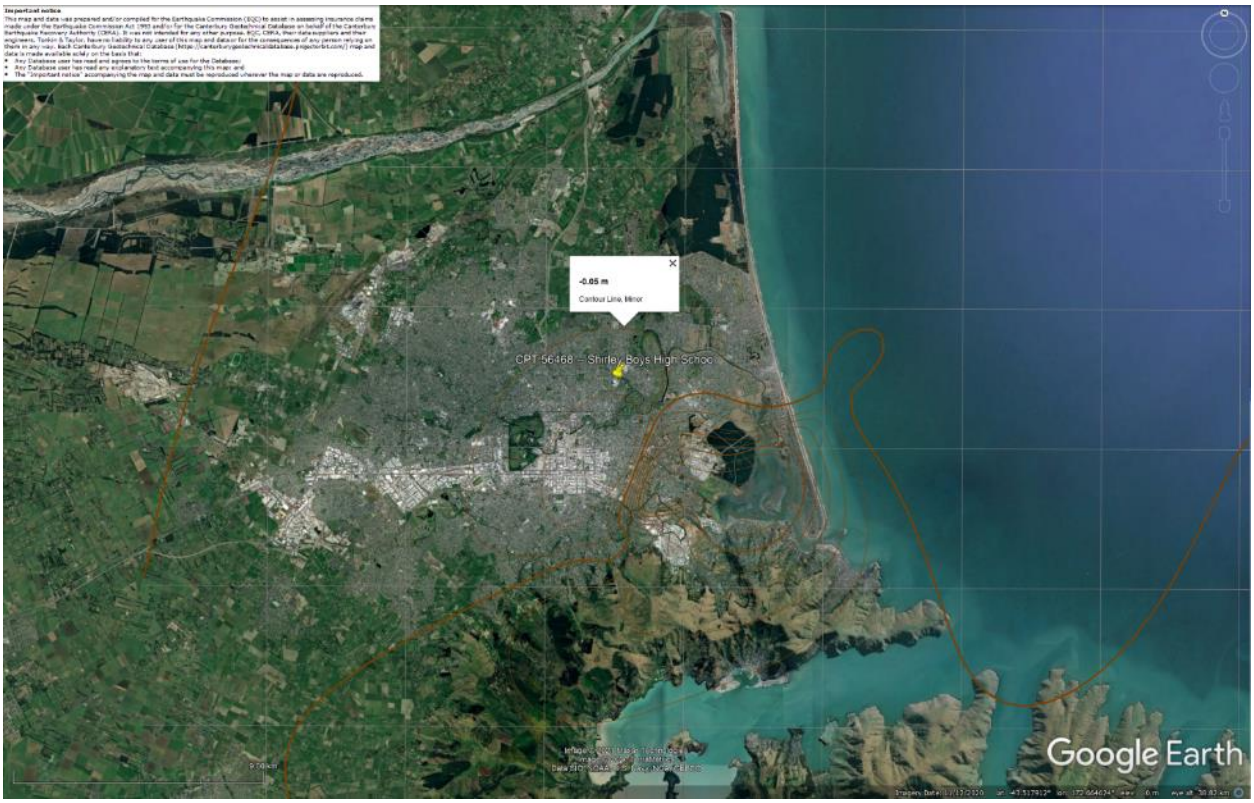

Figure 37: Vertical tectonic movements for Feb 2011 Earthquake.

Figure 38: Vertical tectonic movements for June 2011 Earthquake.

Figure 39: Vertical tectonic movements for Dec 2011 Earthquake.

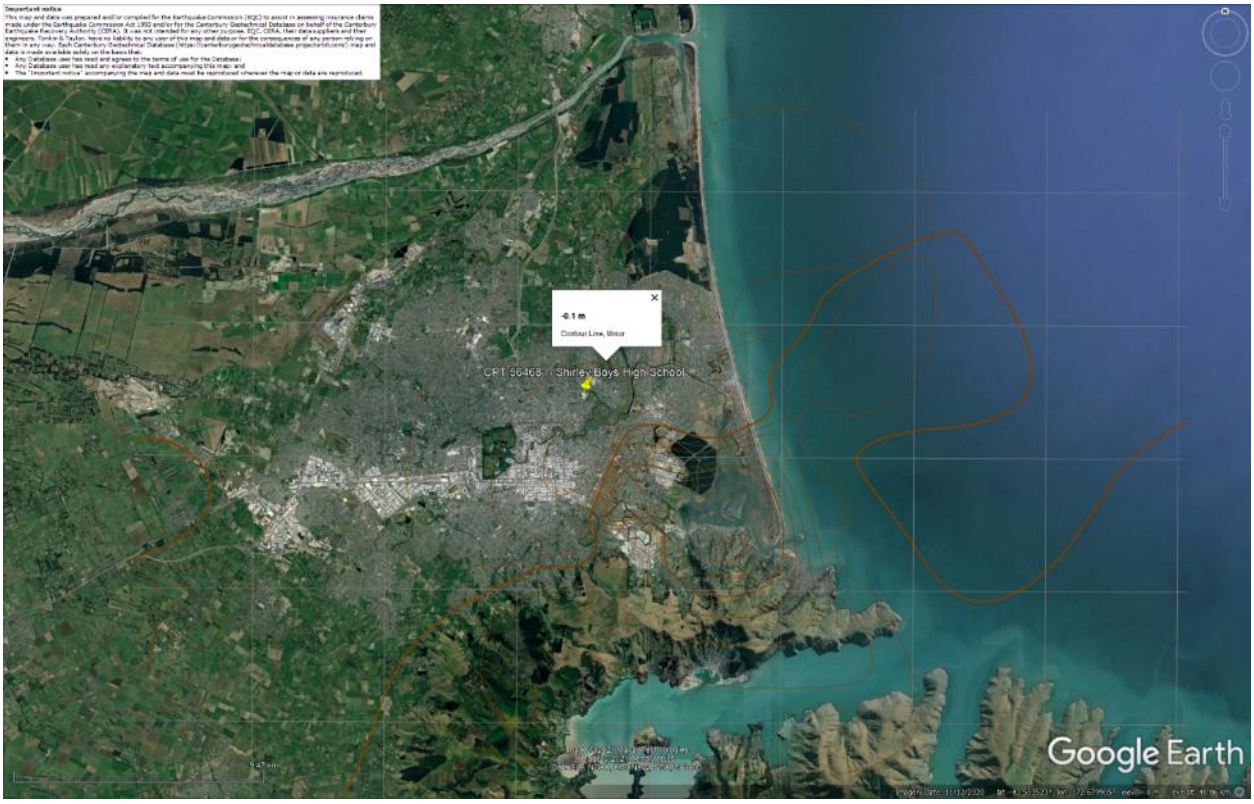

Figure 40: Vertical tectonic movements for Canterbury Earthquake Sequence.

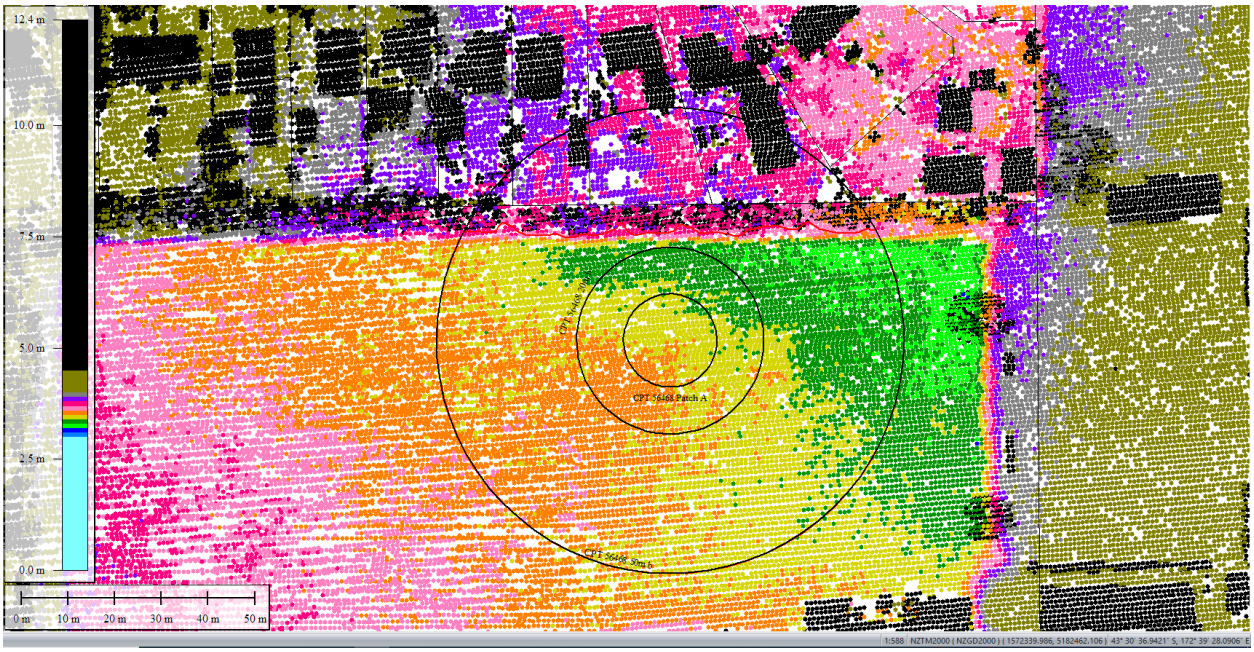

Figure 41: Sep 5, 2010 LiDAR survey.

Figure 42: Ground surface elevation averaged over 10-m buffer for Patch A for Sep 5, 2010 LiDAR survey.

Figure 43: Ground surface elevation averaged over 20-m buffer for Patch A for Sep 5, 2010 LiDAR survey.

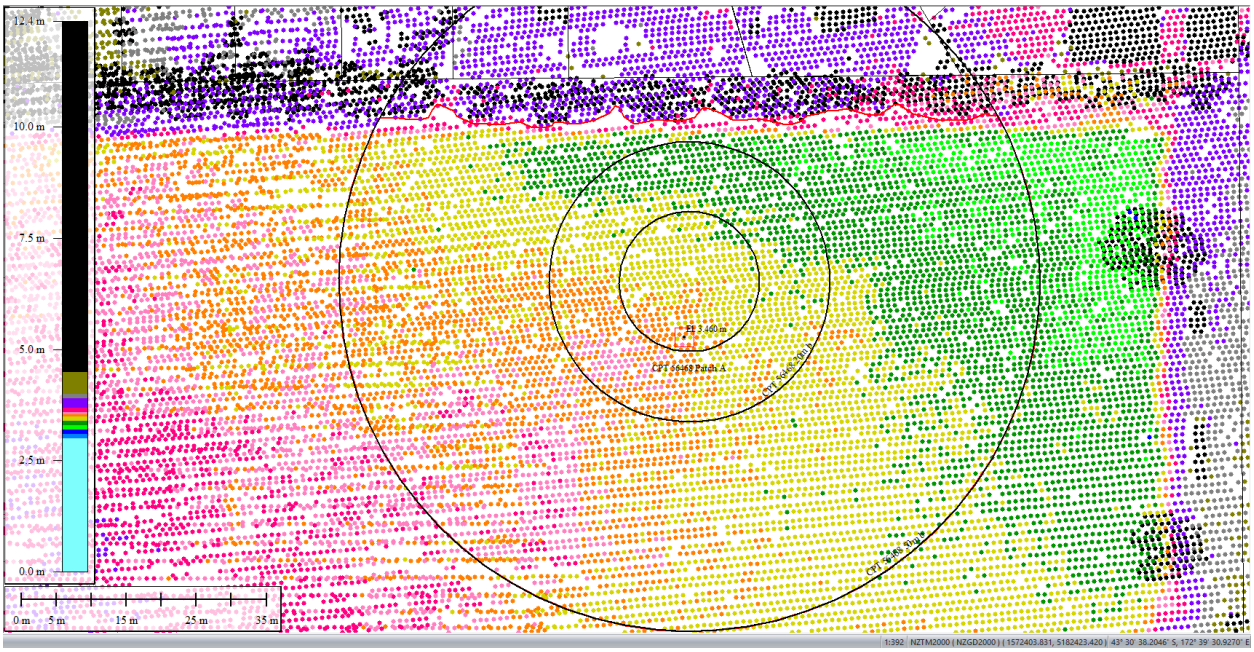

Figure 44: Ground surface elevation averaged over 50-m buffer for Patch A for Sep 5, 2010 LiDAR survey.

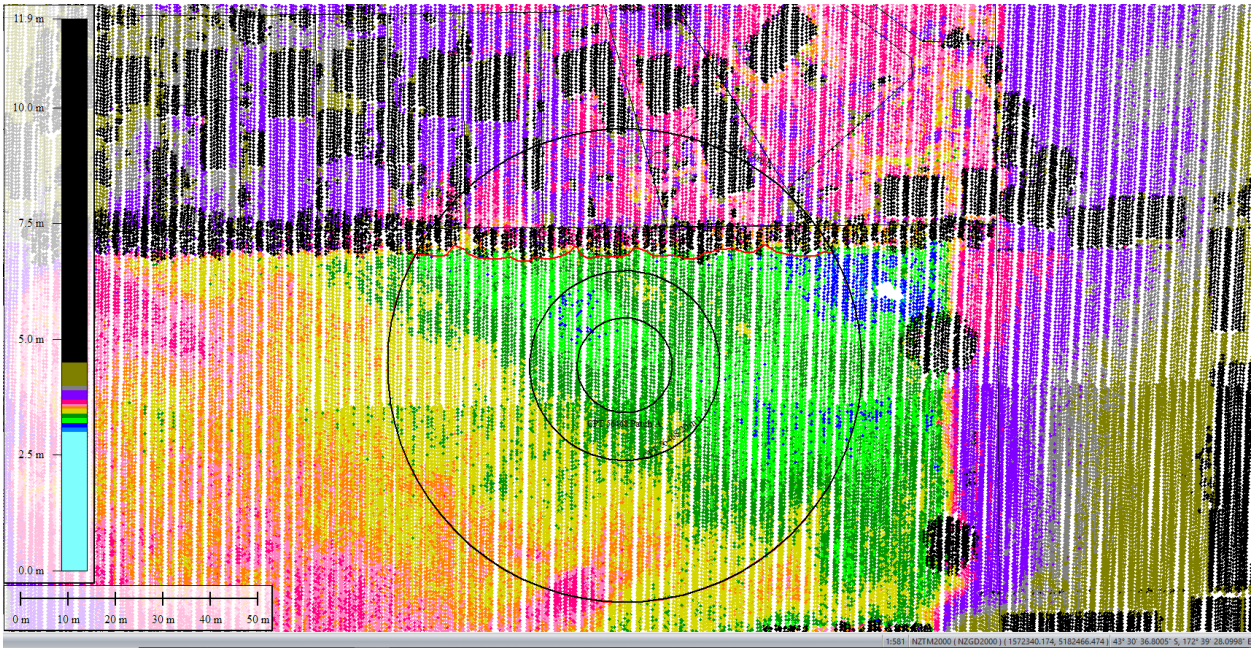

Figure 45: Mar 2011 LiDAR survey.

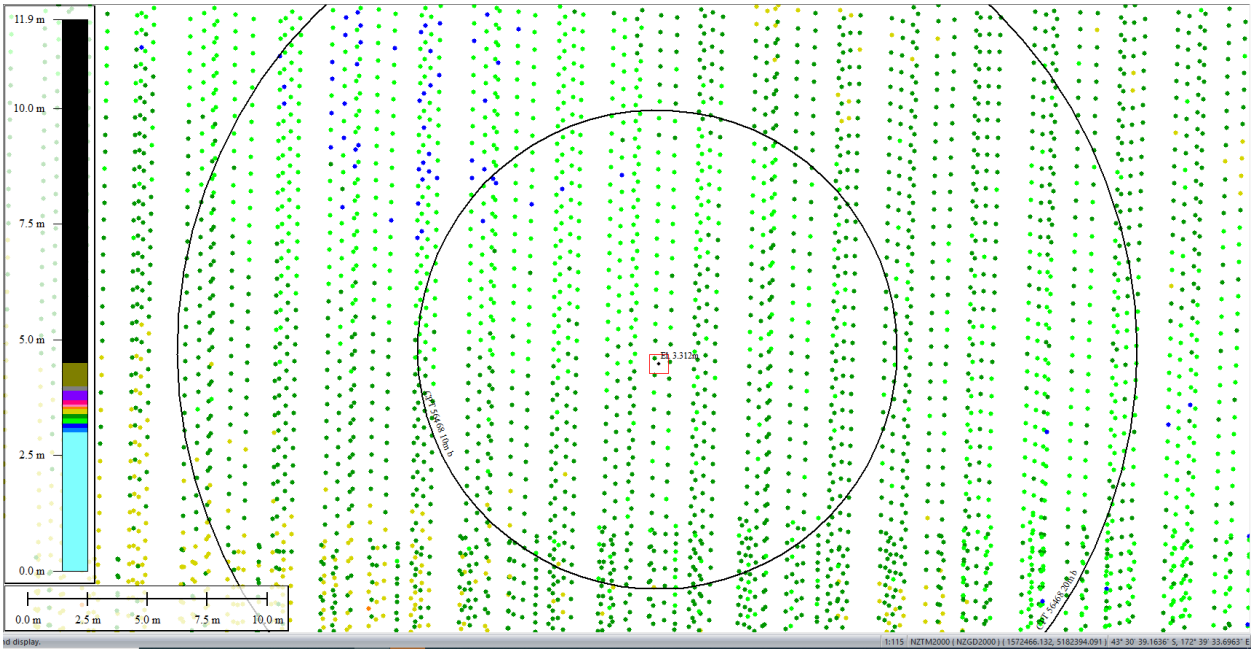

Figure 46: Ground surface elevation averaged over 10-m buffer for Patch A for Mar 2011 LiDAR survey.

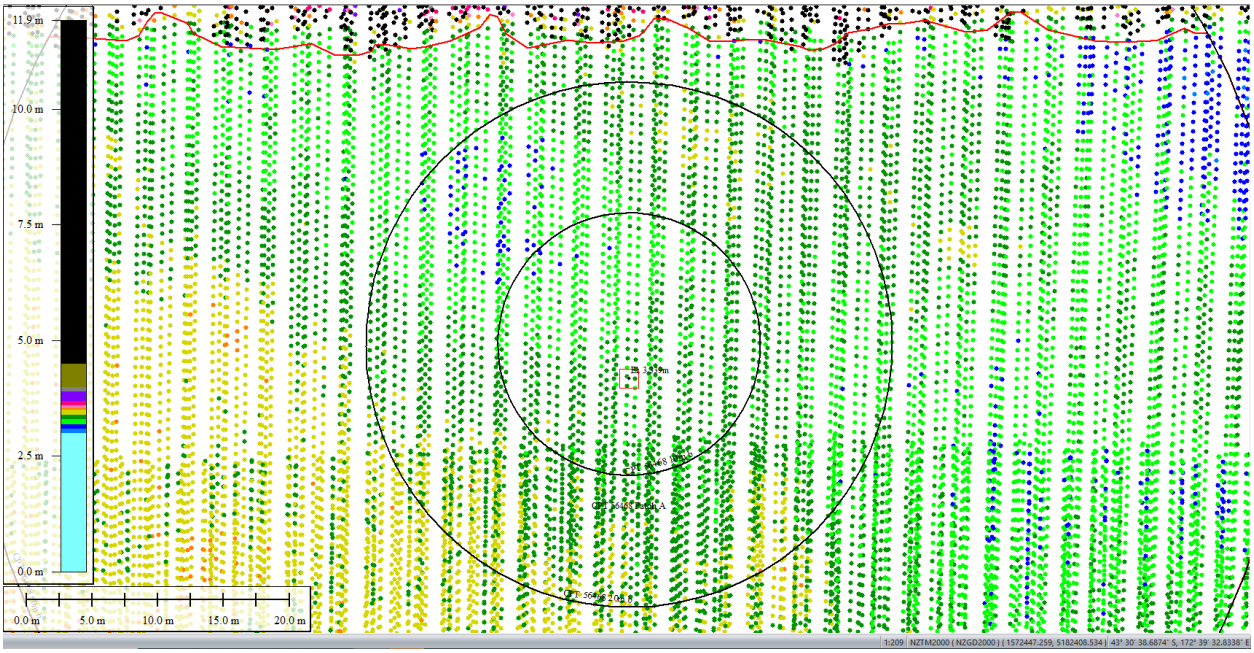

Figure 47: Ground surface elevation averaged over 20-m buffer for Patch A for Mar 2011 LiDAR survey.

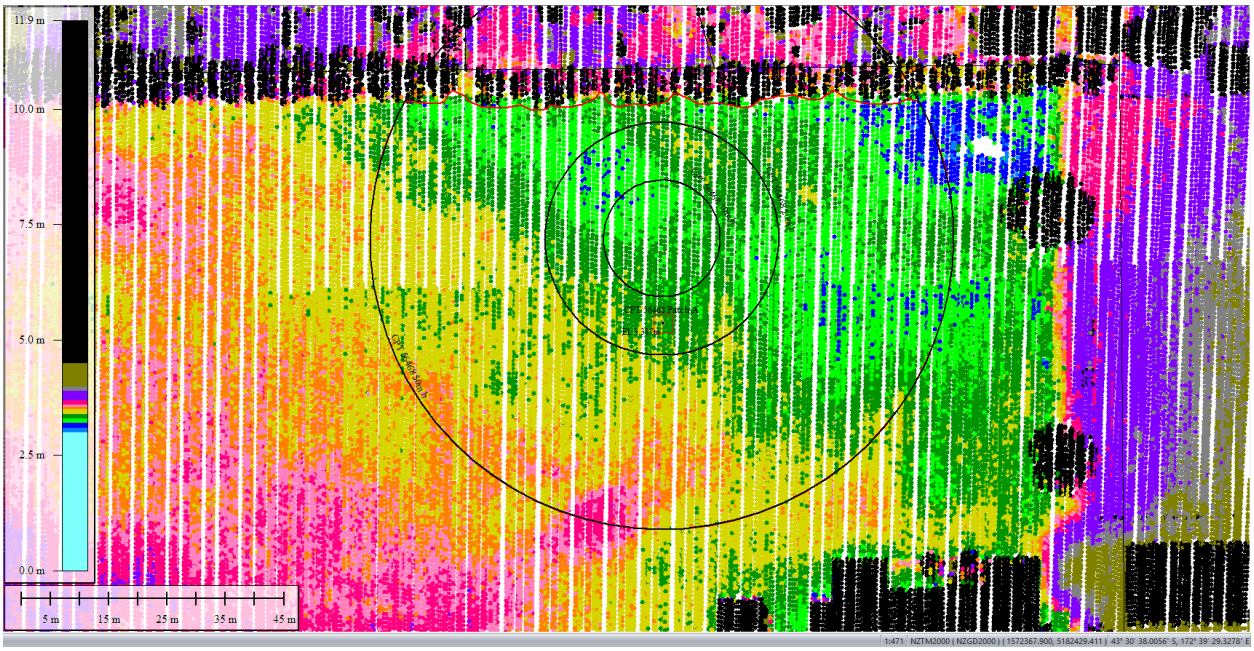

Figure 48: Ground surface elevation averaged over 50-m buffer for Patch A for Mar 2011 LiDAR survey.

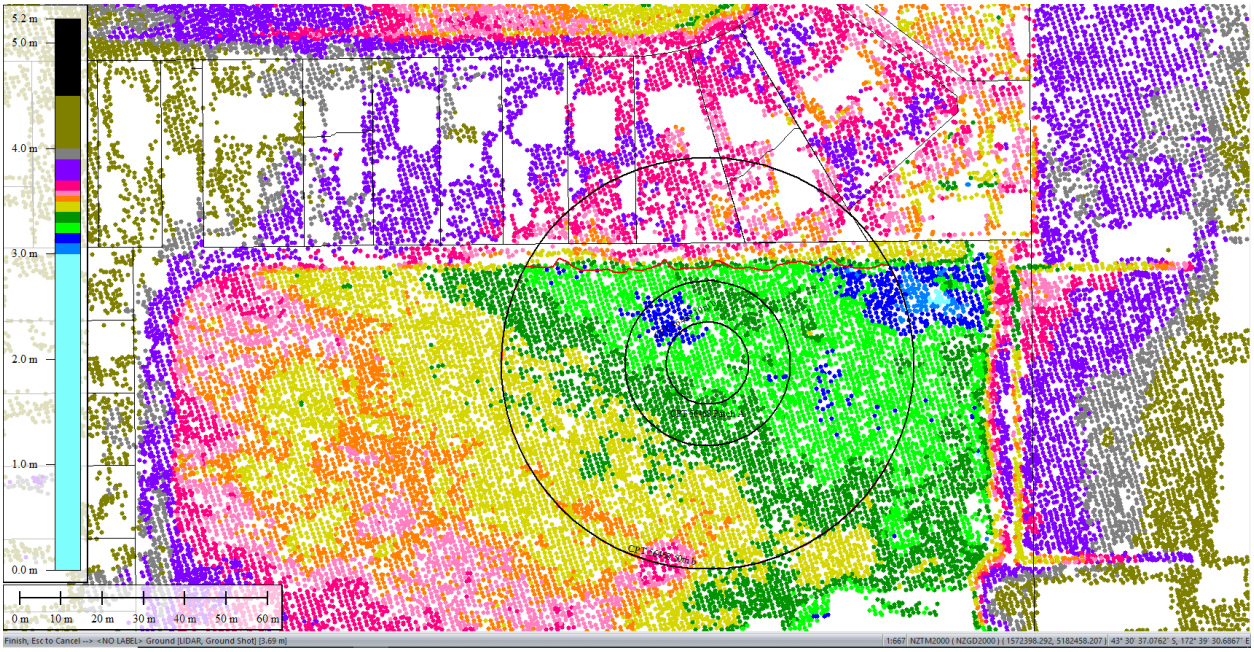

Figure 49: May 2011 LiDAR survey.

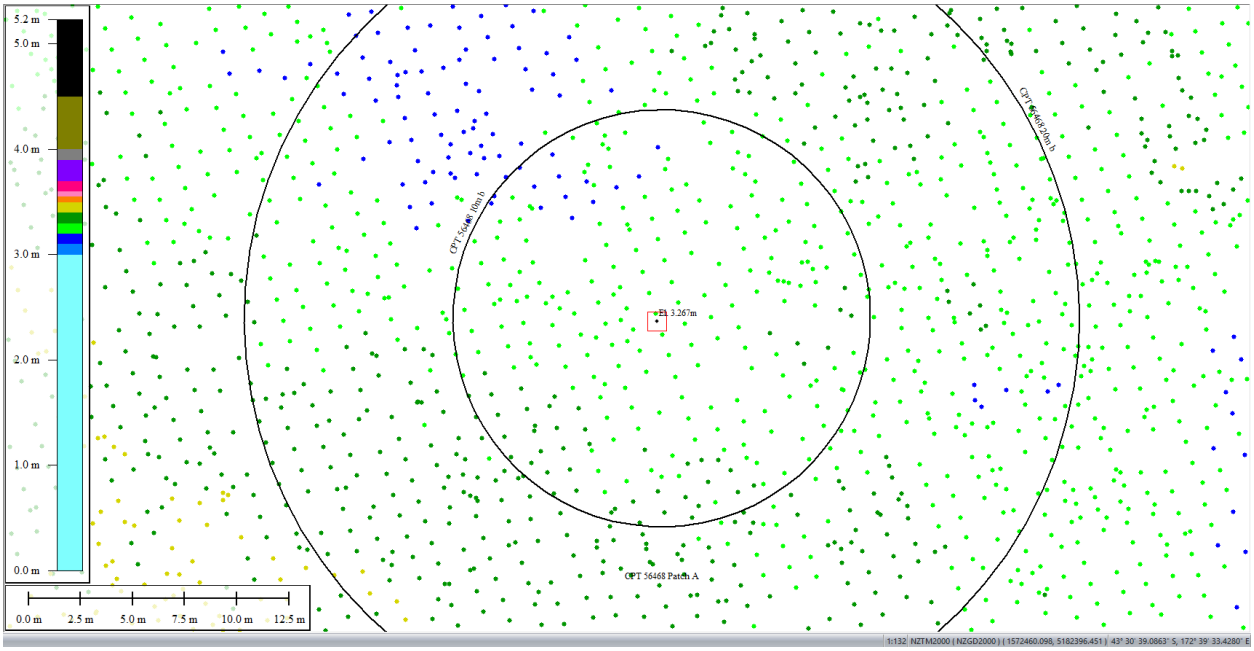

Figure 50: Ground surface elevation averaged over 10-m buffer for Patch A for May 2011 LiDAR survey.

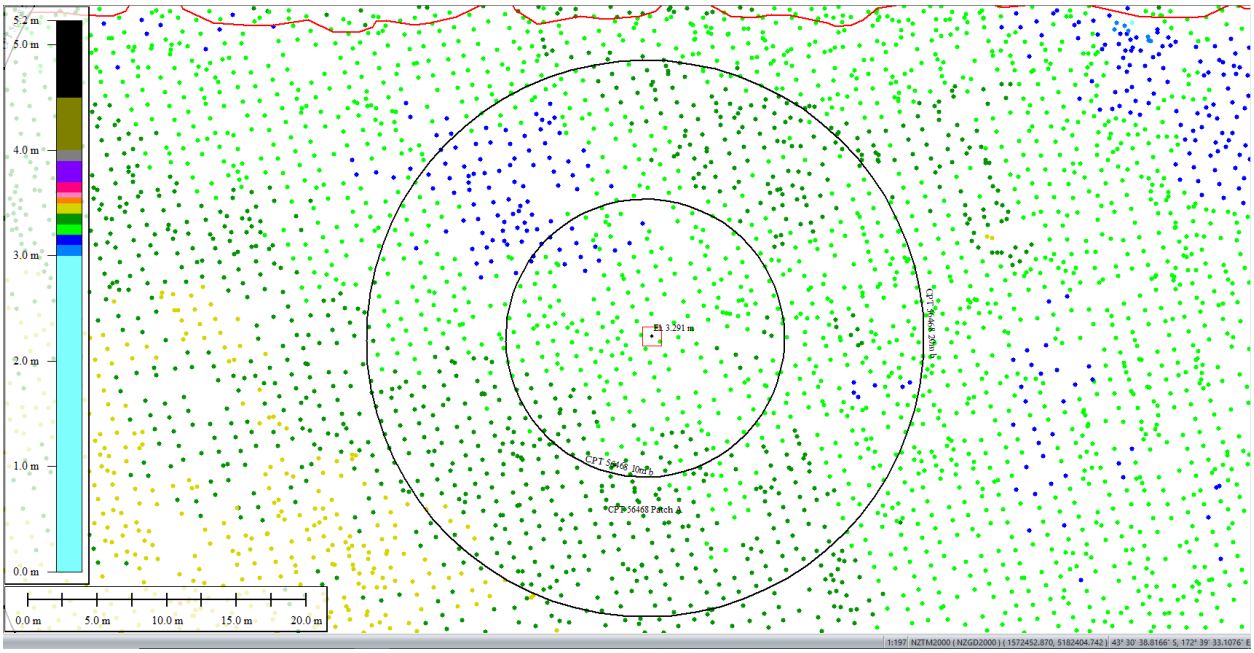

Figure 51: Ground surface elevation averaged over 20-m buffer for Patch A for May 2011 LiDAR survey.

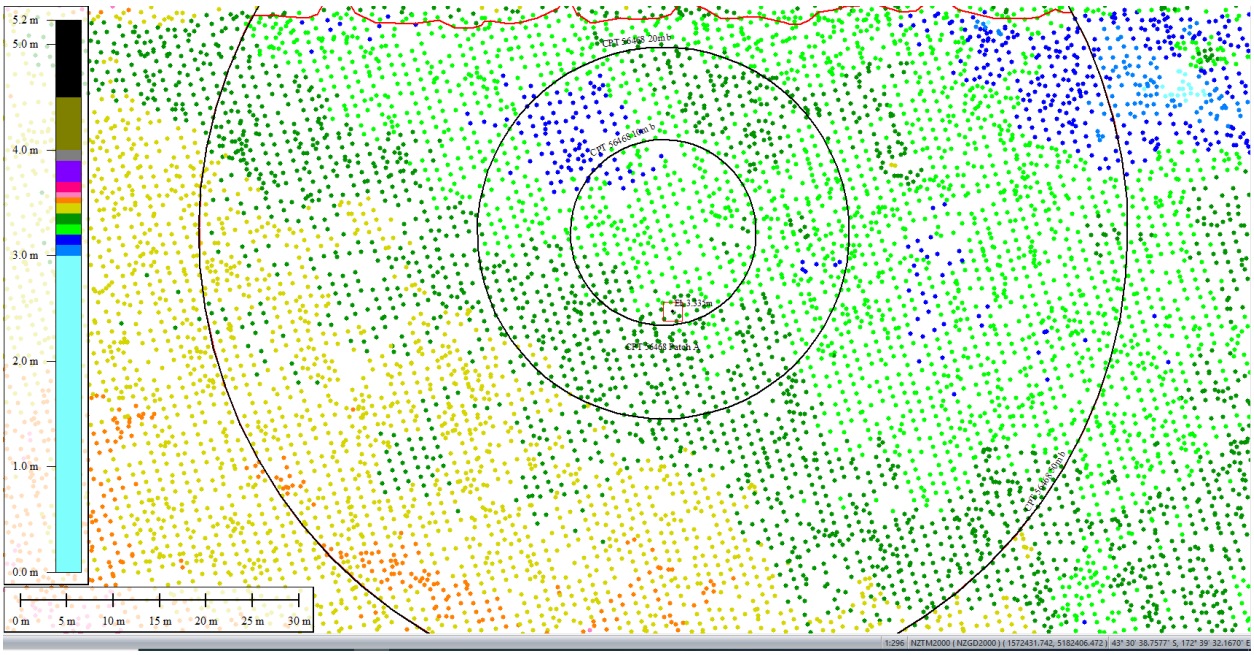

Figure 52: Ground surface elevation averaged over 50-m buffer for Patch A for May 2011 LiDAR survey.

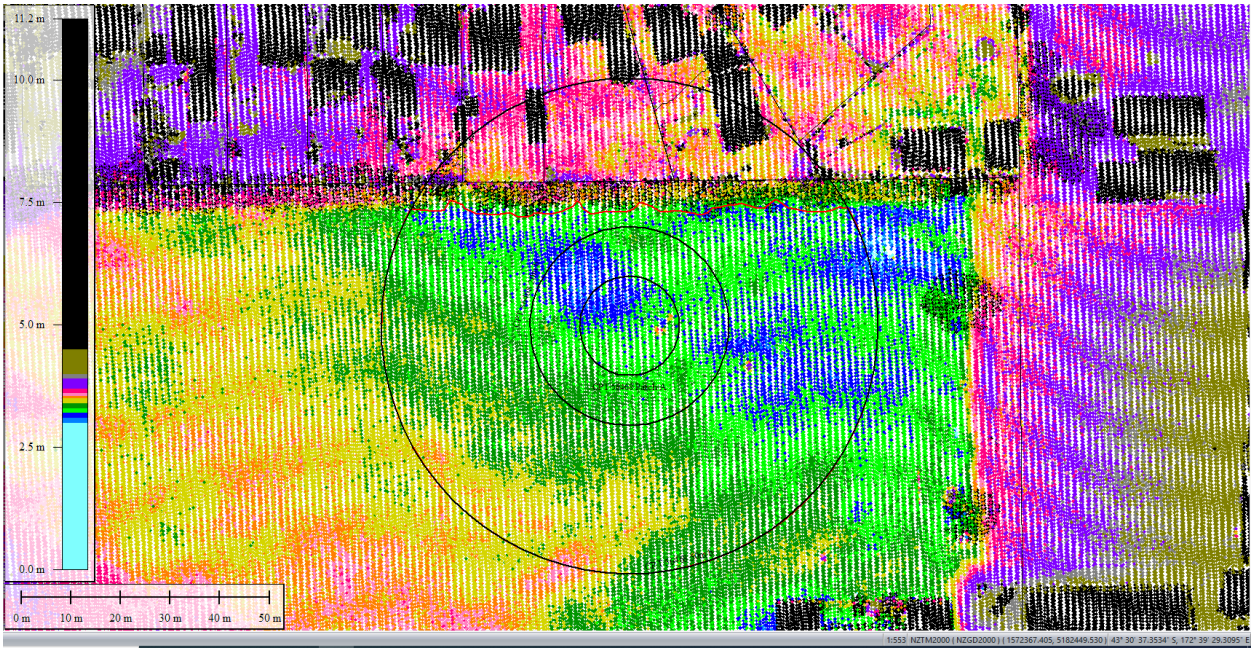

Figure 53: Sep 2011 LiDAR survey.

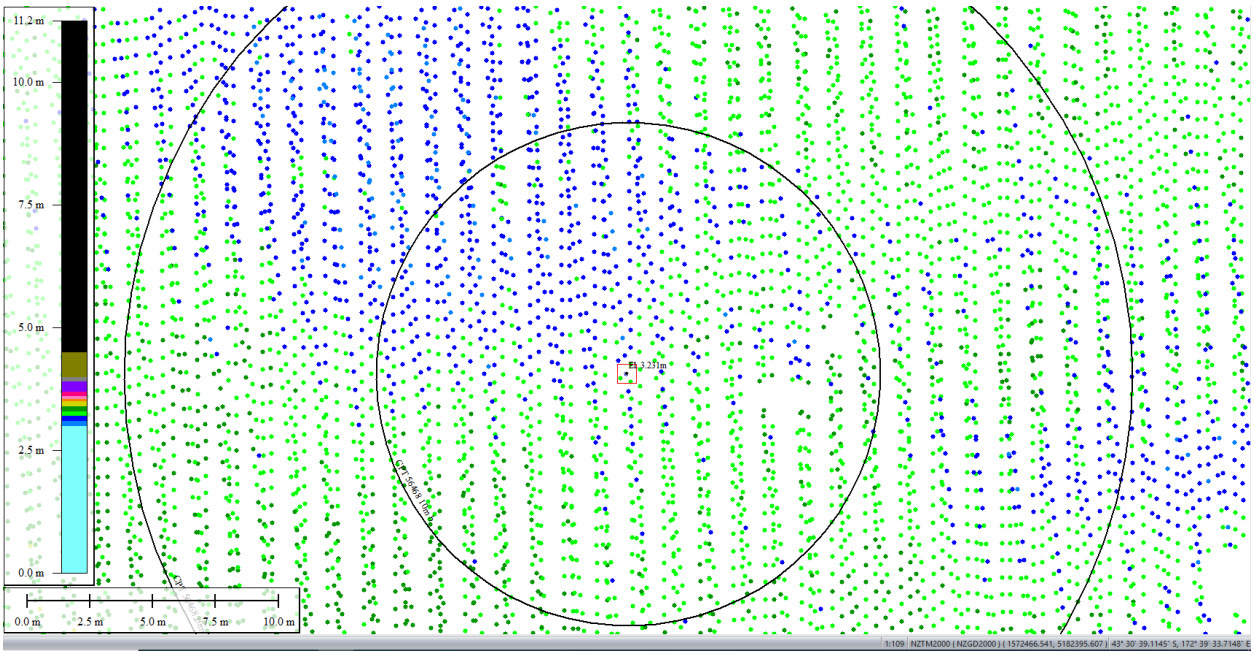

Figure 54: Ground surface elevation averaged over 10-m buffer for Patch A for Sep 2011 LiDAR survey.

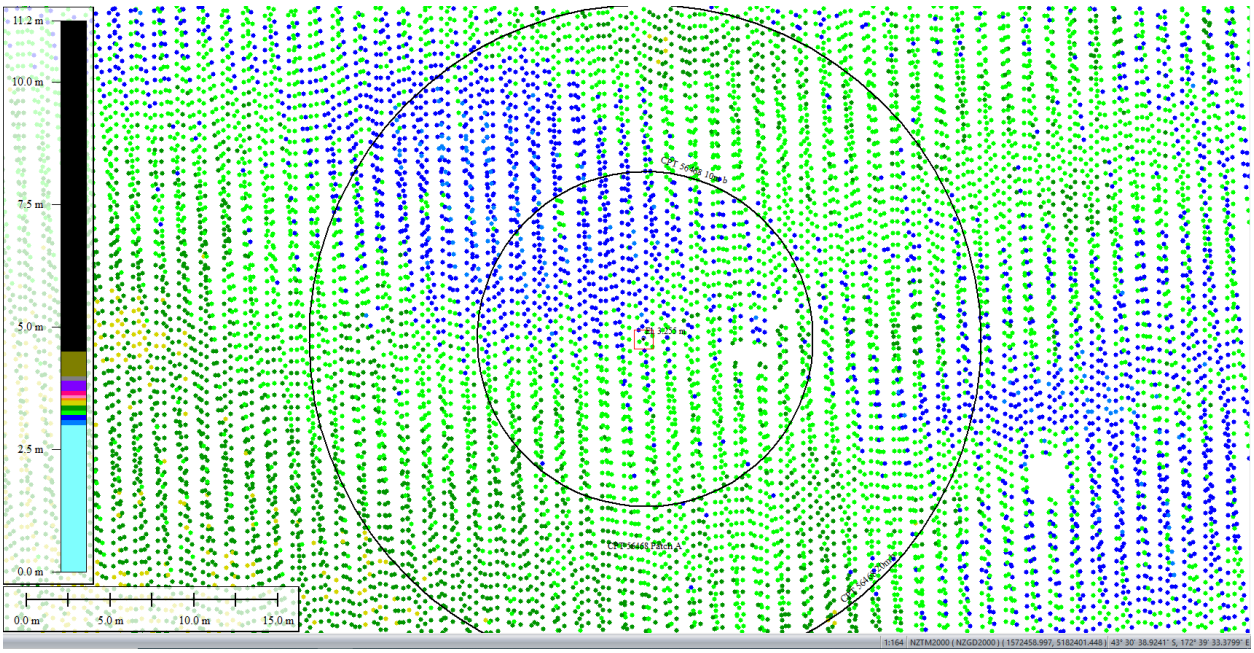

Figure 55: Ground surface elevation averaged over 20-m buffer for Patch A for Sep 2011 LiDAR survey.

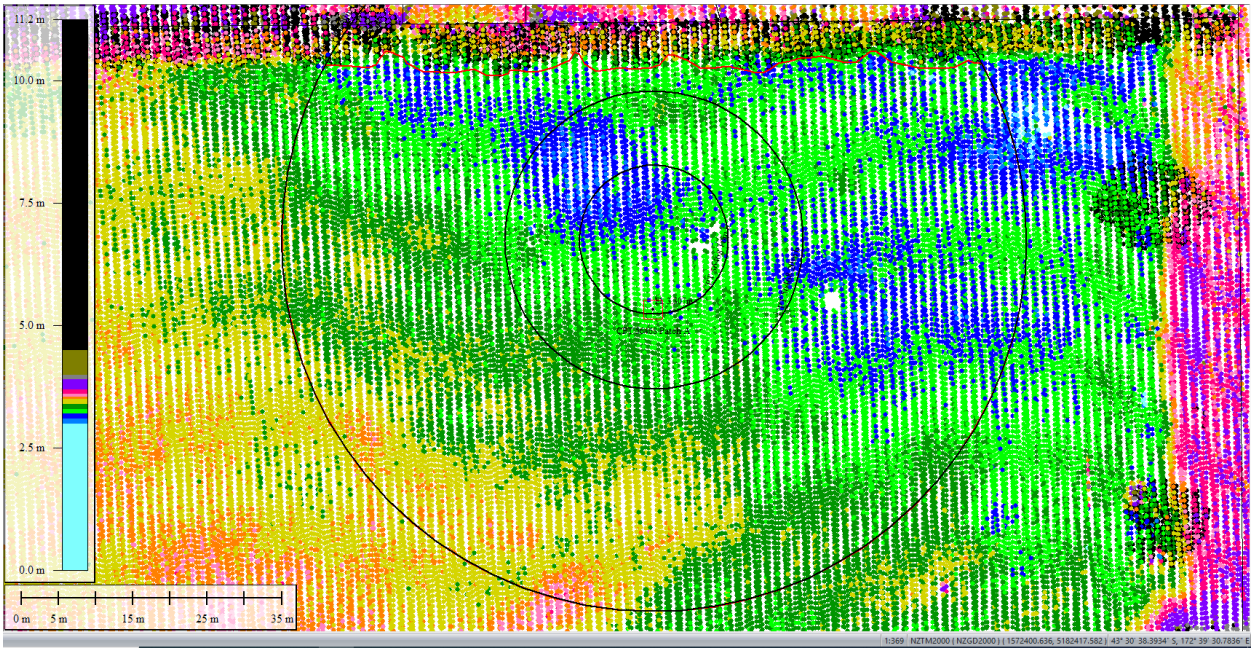

Figure 56: Ground surface elevation averaged over 50-m buffer for Patch A for Sep 2011 LiDAR survey.

Figure 57: Aerial photograph showing the ejecta outline at the site for Feb-11 EQ.

Figure 58: Aerial photograph acquired on 16 Jun 2011 showing the ejecta outline at the site for Jun-11 EQ.

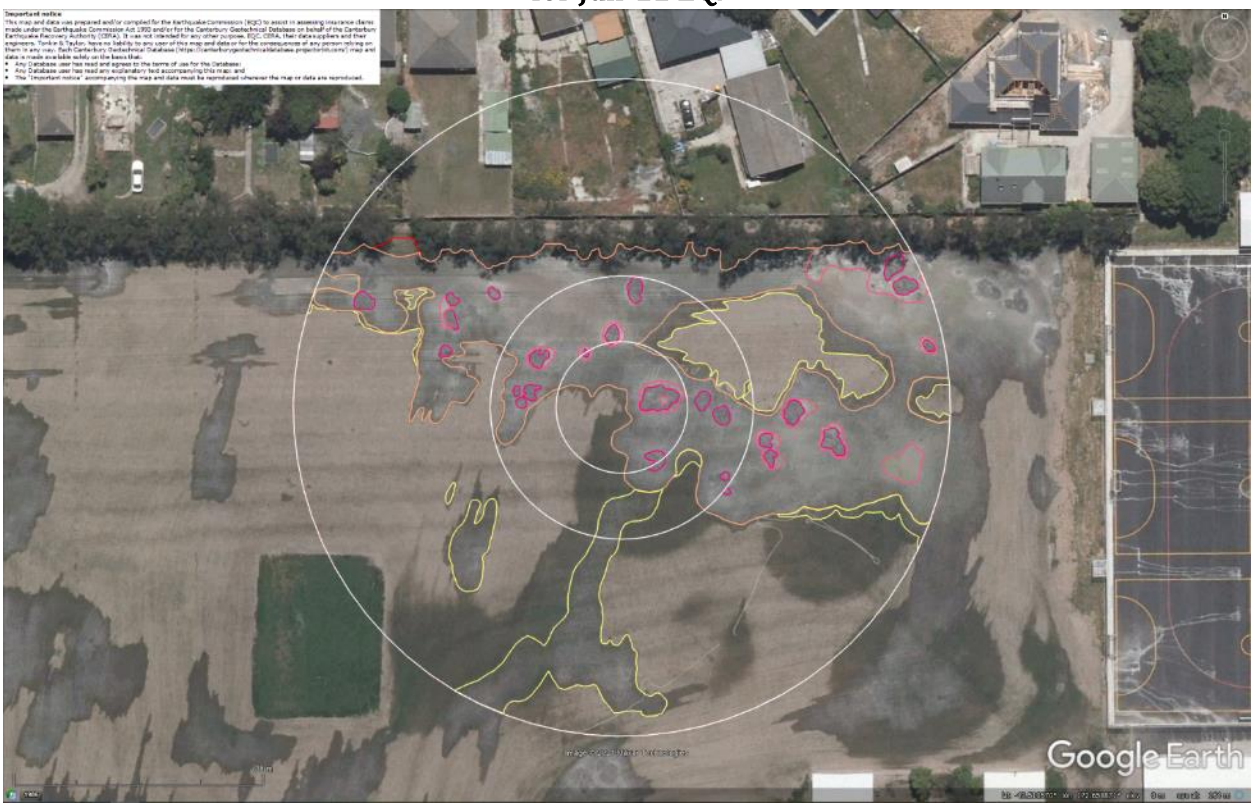

Figure 59: Aerial photograph showing the ejecta outline at the site for Dec-11 EQ.

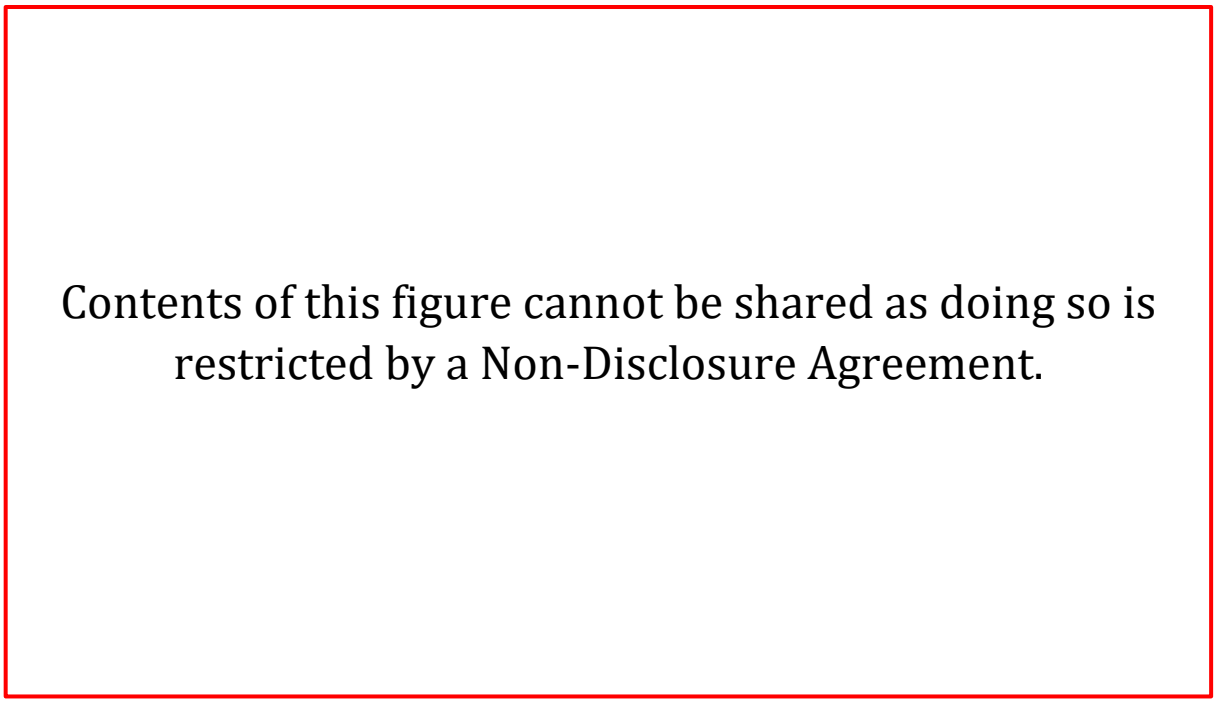

Figure 60: LDAT inspection report for the property in the N portion of the 50-m buffer (inspection date: May 2011).

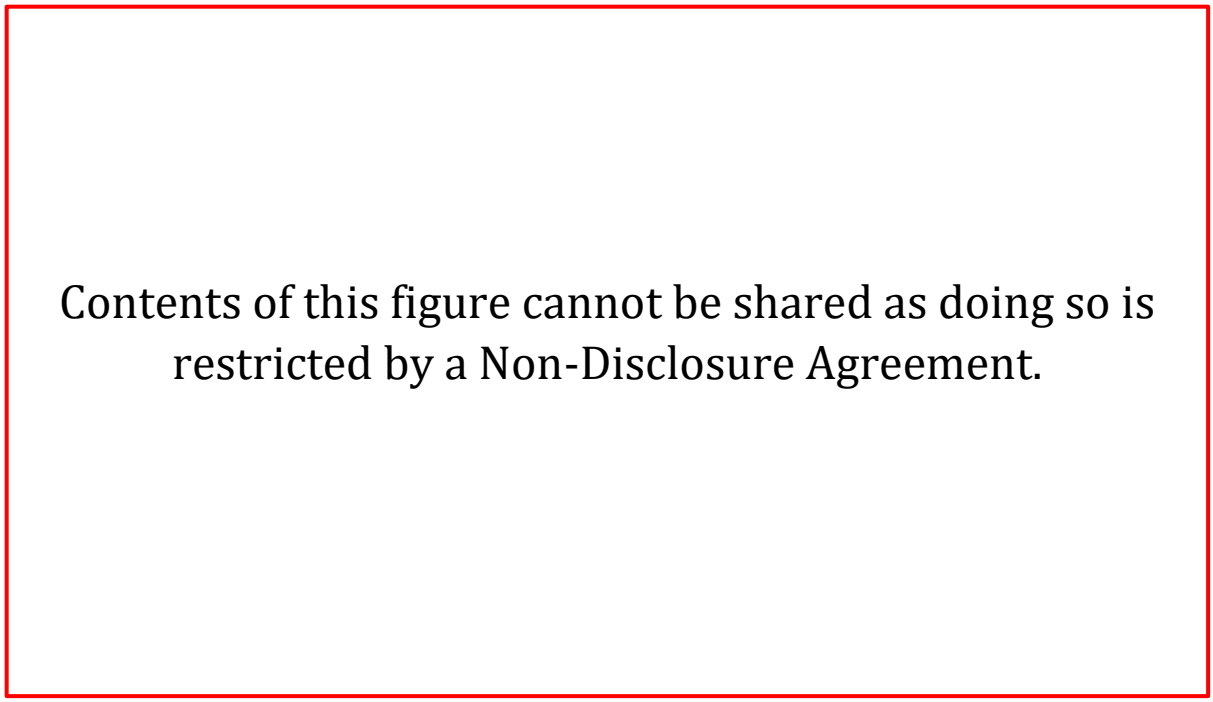

Figure 61: LDAT inspection report for the property in the NE portion of the 50-m buffer (inspection date: May 2011).

Figure 62: Ground photographs showing ejecta remnants at the properties within the 50-m buffer (photograph date: May 2011).

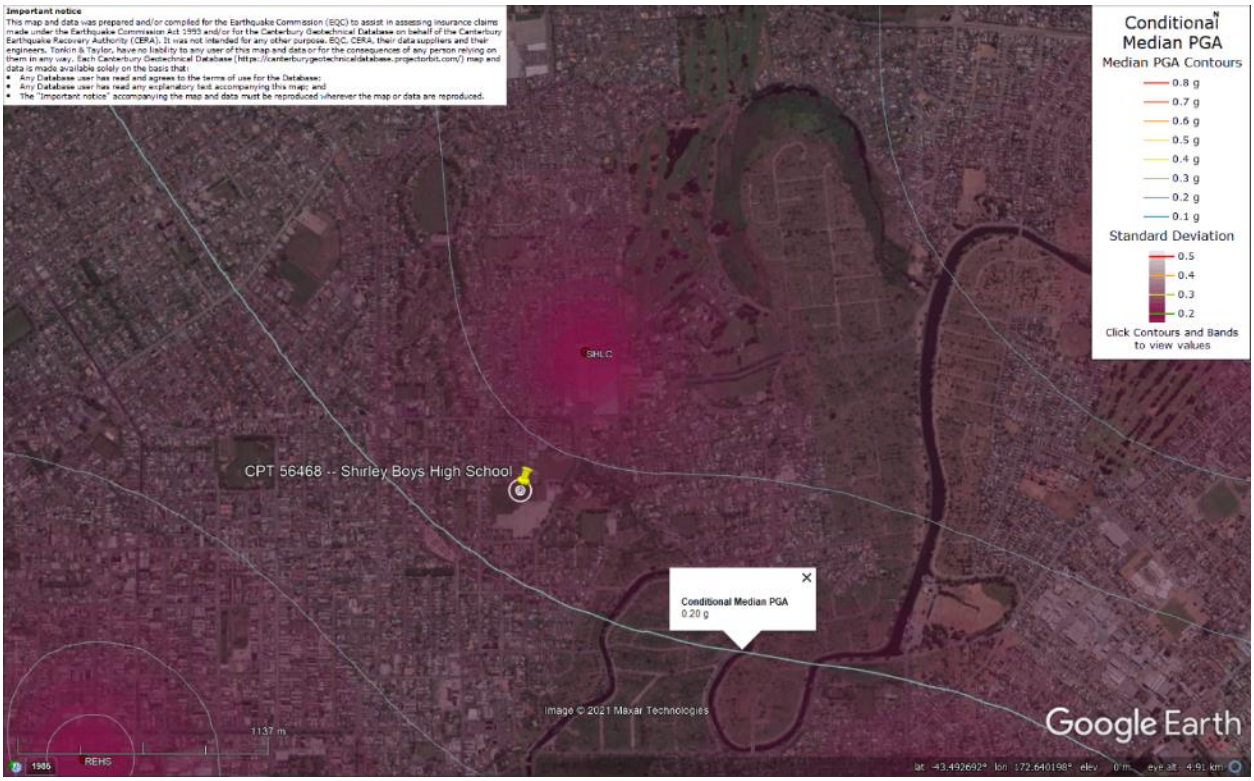

Figure 63: PGA for Sep-10 EQ (st. dev. = 0.250-0.300 ln units).

Figure 64: PGA for Feb-11 EQ (st. dev. = 0.275-0.300 ln units).

Figure 65: PGA for Jun-11 EQ (st. dev. = 0.0.300-0.325 ln units).

Figure 66: PGA for Dec-11 EQ (st. dev. = 0.300-0.325 ln units).

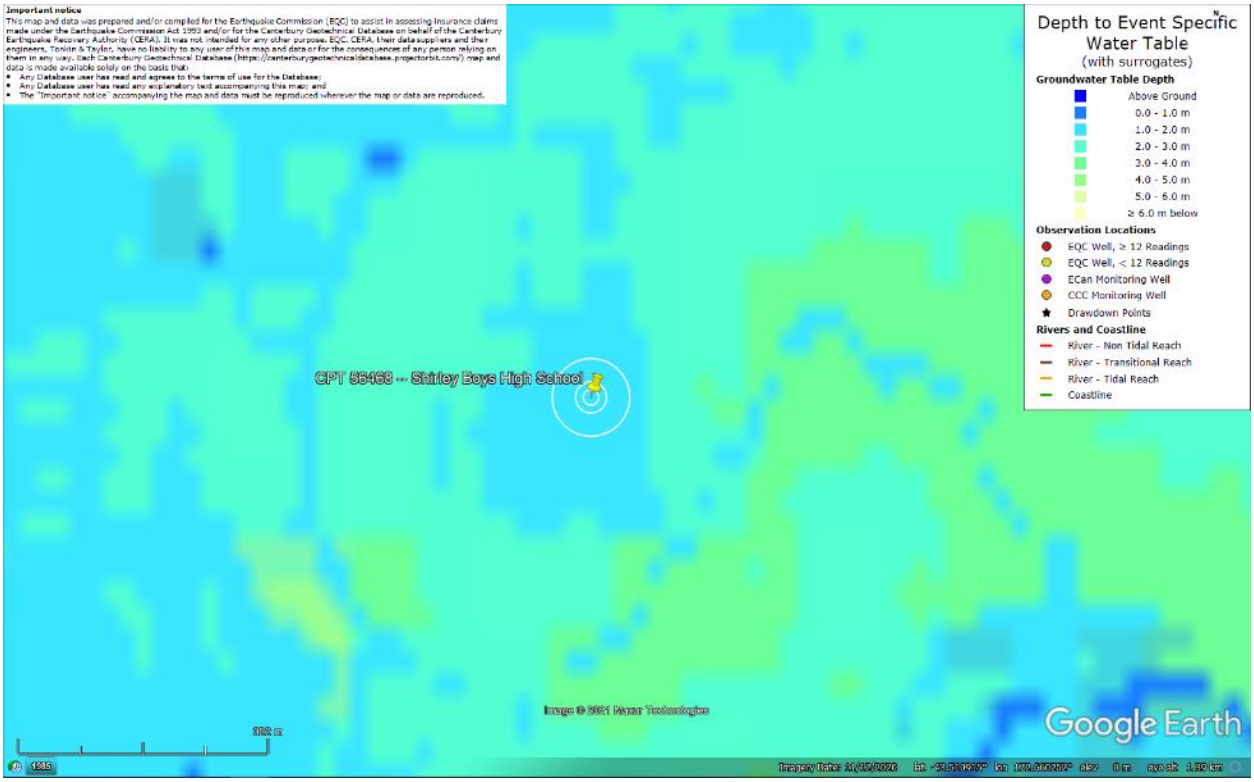

Figure 67: Depth to groundwater table for Sep-10 EQ.

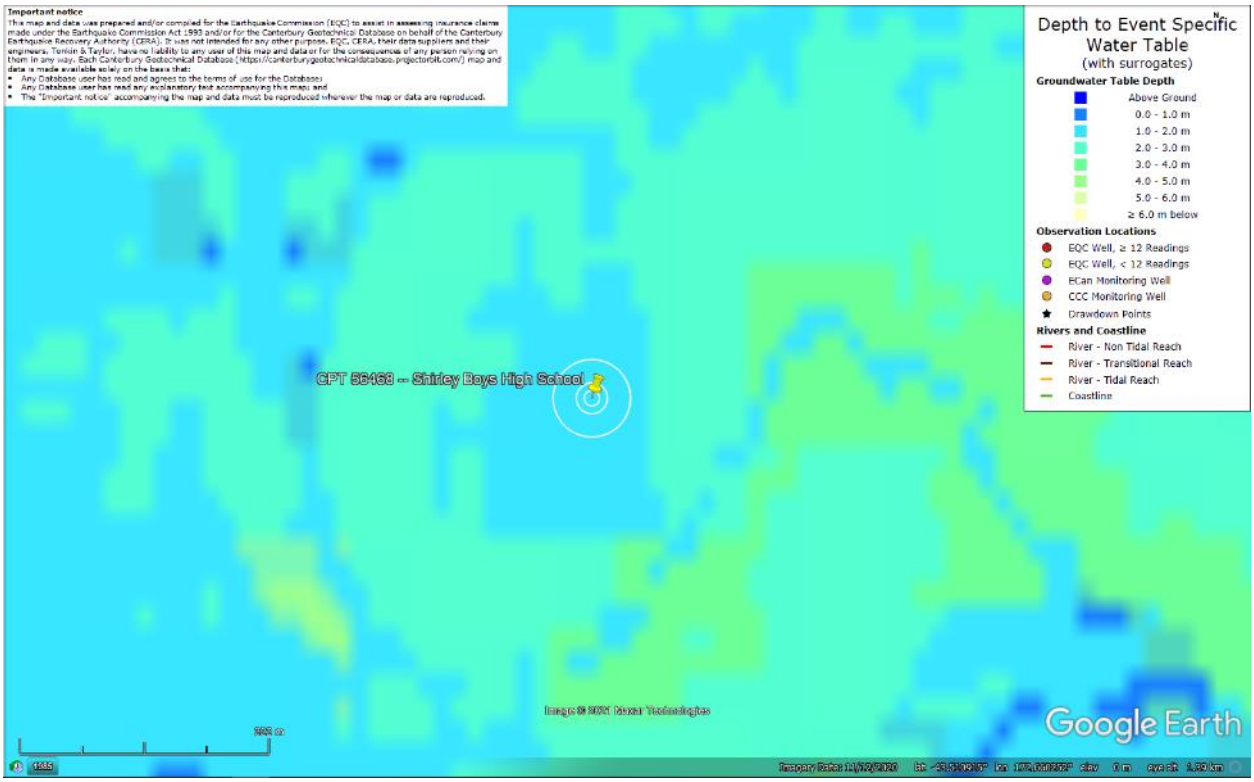

Figure 68: Depth to groundwater table for Feb-11 EQ.

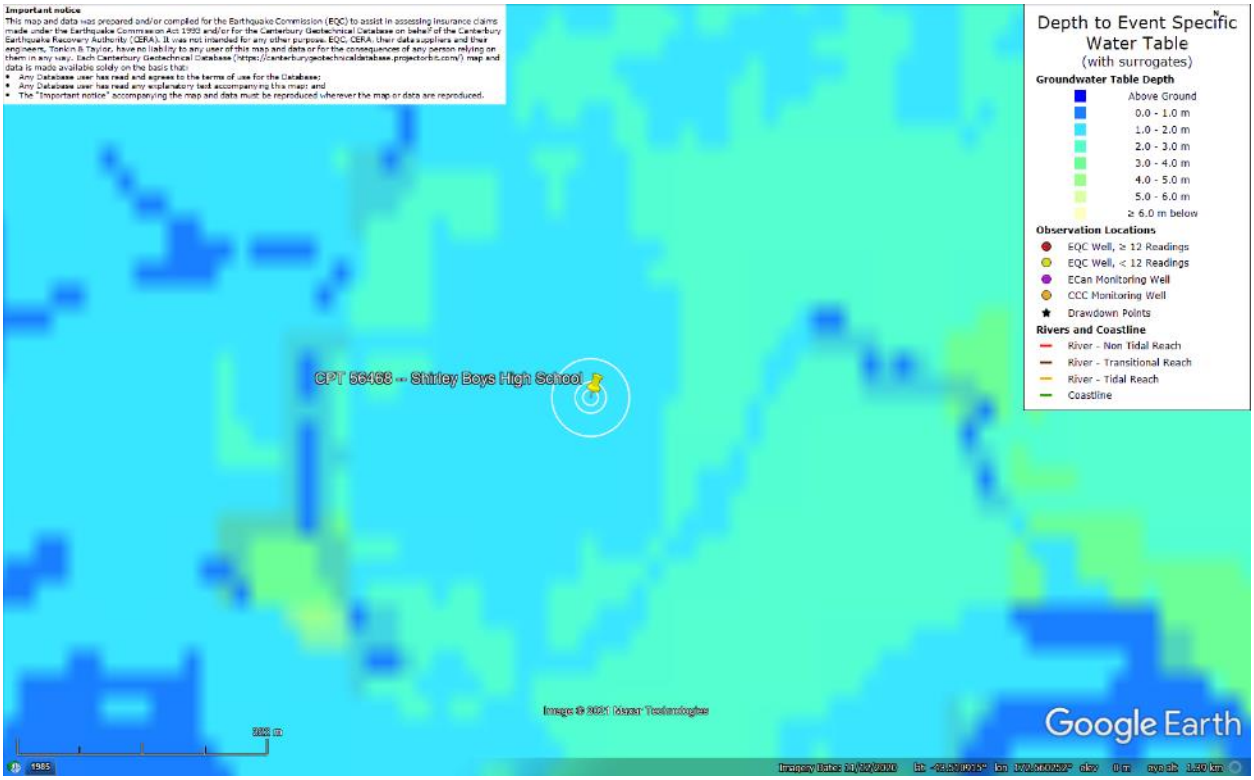

Figure 69: Depth to groundwater table for Jun-11 EQ.

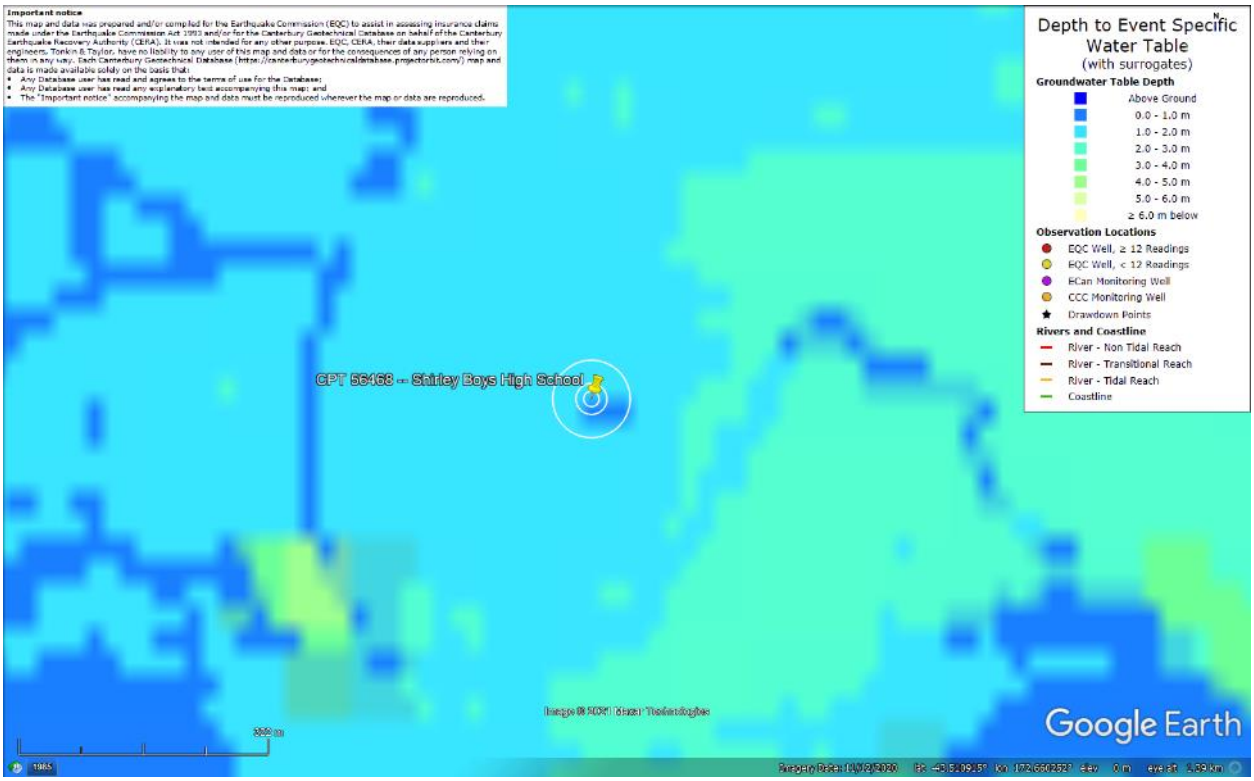

Figure 70: Depth to groundwater table for Dec-11 EQ.

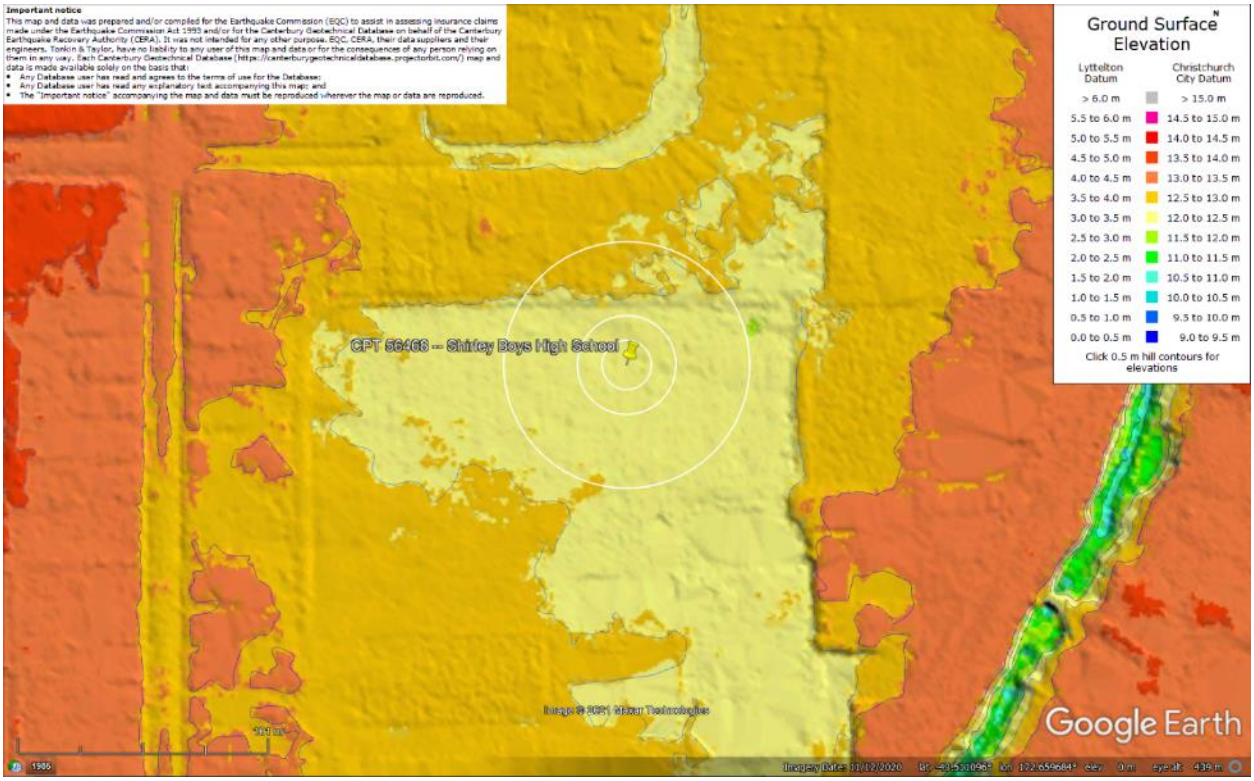

Figure 71: Ground surface elevation according to the Sep-11 LiDAR survey.

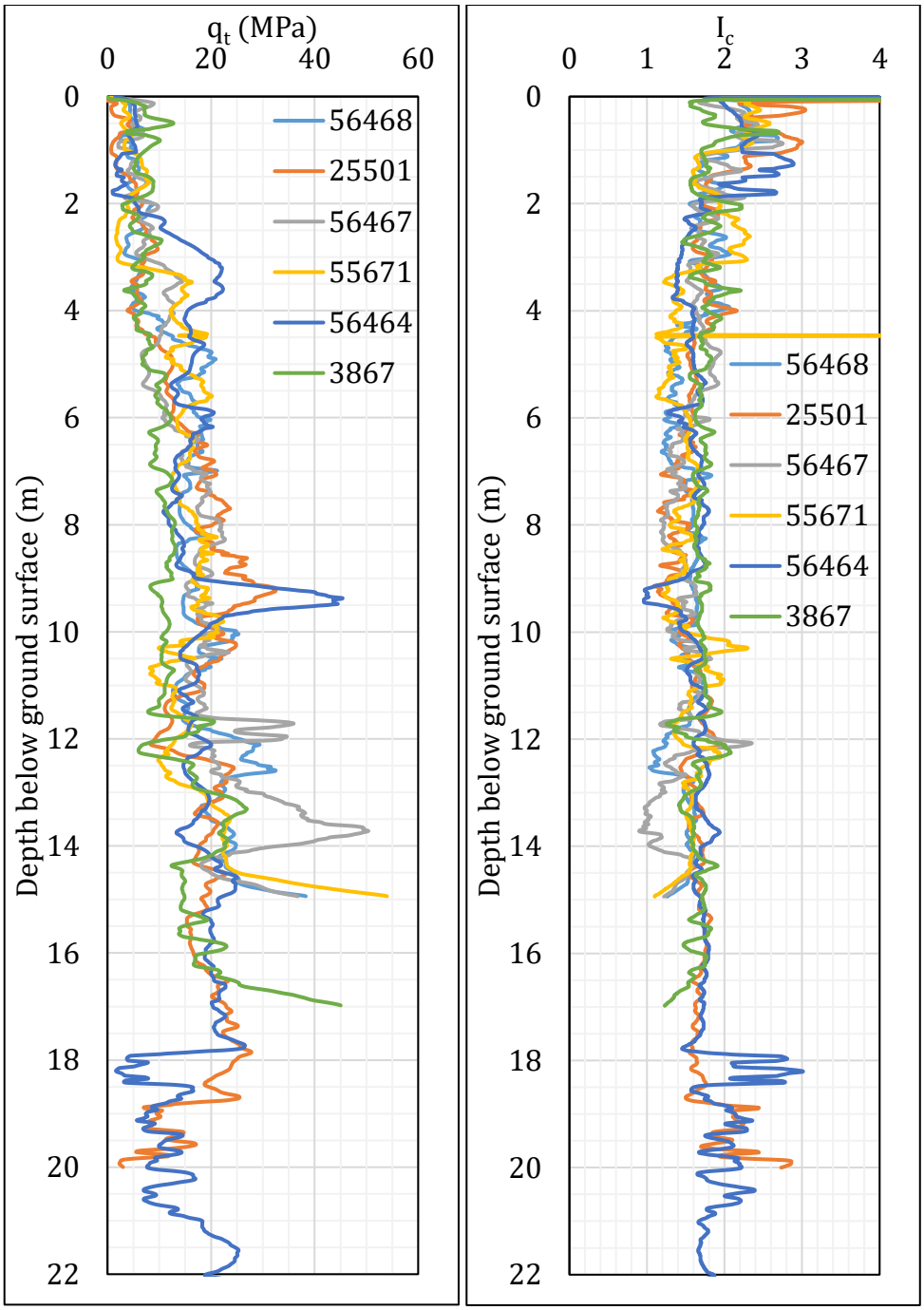

Figure 72: q_t and I_c profiles.

Note 6: The selection of CPTs for the area considered for settlement assessment (Figure 1) is based on the proximity of the CPTs to the considered areas. In accordance with that, the following table shows CPTs that were used for the volumetric settlement analysis in *Cliq v.3.0.3.2*, a CPT soil liquefaction software developed by GeoLogismiki. (The average volumetric settlements were reported in Table 8.)

Table 12: CPT profiles used in volumetric settlement analysis for areas selected for settlement assessment.

CPT ID No.	10-m buffer	20-m buffer	50-m buffer
56468	✓	✓	✓
25501			✓
56467			✓
55671			✓
56464			
3867			✓

Note: CPTs 25501 and 56464 were used to compute the volumetric settlement for CPTs 56468, 56467, and 55671 for a depth range from 14.9 m to 20 m and CPT 3867 for a depth range from 17.0 m to 20 m.

Table 13: CPT-based results.

		CPT ID							
EQ Event	Parameter	56468	25501	56467	55671	56464	3867	$\Delta_{14.9m-20m}$	$\Delta_{16.7m-20m}$
Sep-10	S_{V1D} (mm)	9	9	2	25	11	41	6	6
	LSN	3	1	0	5	1	6	1	1
	LPI	0	0	0	0	0	0	0	0
	LPI_{ish}	0	0	0	0	0	0	--	--
	$D_{FS<1}$ (m)	undet.	undet.	undet.	2.58	undet.	9.23	--	--
Feb-11	S_{V1D} (mm)	64	55	35	73	54	181	19	19
	LSN	19	12	9	17	10	31	1	1
	LPI	6	4	3	7	2	17	0	0
	LPI_{ish}	6	2	2	6	3	9	--	--
	$D_{FS<1}$ (m)	1.51	1.52	2.48	1.84	1.52	1.95	--	--
Jun-11	S_{V1D} (mm)	8	4	1	21	6	27	2	2
	LSN	2	1	0	5	1	4	0	0
	LPI	0	0	0	0	0	0	0	0
	LPI_{ish}	0	0	0	0	0	0	--	--
	$D_{FS<1}$ (m)	undet.	undet.	undet.	2.57	undet.	undet.	--	--
Dec-11	S_{V1D} (mm)	25	17	7	42	16	69	6	6
	LSN	9	5	2	11	4	12	1	1
	LPI	1	0	0	2	0	2	0	0
	LPI_{ish}	1	0	0	2	0	0	--	--
	$D_{FS<1}$ (m)	2.63	undet.	undet.	2.27	undet.	4.22	--	--

Notes: $D_{FS<1}$ = Depth to the first liquefiable layer ($FS_L<1$) that is at least 200-mm thick, as determined by the Boulanger and Idriss (2016) liquefaction-triggering procedure (P_L=50%, C_{FC}=0.13, and $I_{c,cutoff}$ =2.6), and exported from *Cliq v.3.0.3.2*; undet. = the specified soil layer was not detected; $\Delta_{14.9m-20m}$ and $\Delta_{16.7m-20m}$ indicate the amount of SV1D, LSN, and LPI added to CPTs 56468, 56467, and 55671 and CPT 3867, respectively, due to their penetration depths being shallower than 20 m.

Note 7: Based on the borehole log (BH 62337, Figure 1), the groundwater table is at a depth of 1.8 m below the ground surface. The soil profile consists of (1) topsoil to a depth of 0.5 m, (2) silt, ML, the Yaldhurst member of the Springston formation, to a depth of 1.9 m, (3) poorly graded sand, SP, intermixed Springston and Christchurch formations, to a depth of 6.4 m, (4) well graded sand, SW, intermixed Springston and Christchurch formations, to a depth of 10.0 m, (5) well graded sand, SW, of the Christchurch formation, to a depth of 14.0 m, (6) poorly graded sand, SP, of the Christchurch formation, to a depth of 20 m. The SP layer extends to a depth of 23.3 m, which is underlain by silt, ML, of the Christchurch formation, to a depth of 24.8 m and peat, Pt, of the Christchurch formation, to a depth of 24.9 m (the end of the borehole).

Note 8: The ejecta-induced free-field settlement provided in Table 11 is an areal average settlement due to ejecta, which is based on the total settlement assessment area, A_T (provided in Table 9 and repeated in Table 14). However, the considered area was not always covered completely with ejecta; thus, it is important to provide the localized ejecta-induced settlement, too. The localized settlement due to ejecta is estimated using photographic evidence only as

$$S_{E,P\_localized} = \frac{V_E}{A_E}$$

where V_E is the total volume of ejecta within A_T and A_E is the total coverage area of ejecta within A_T. Please note that the areal ejecta-induced settlement provided in Table 14 as S_{E,P_areal} is the same as $S_{E,P}$ in Table 11, which was estimated as

$$S_{E,P\_areal} = S_{E,P} = \frac{V_E}{A_T}$$

where V_E is the total volume of ejecta within A_T and A_T is the total settlement assessment area.

Table 14a: Areal and localized ejecta-induced settlement estimates for Patch A (10-m buffer) based on photographic evidence.

Earthquake Event	A_T (m^2)	A_E (m^2)	V_E (m^3)	S_{E,P_areal} (mm)	$S_{E,P\_localized}$ (mm)
Sep-10	314	0	0	0	0
Feb-11	314	314	1.6-3.2	10±5	10±5
Jun-11	314	282	4.8-8.4	20±5	25±5
Dec-11	314	204	3.2-6.4	15±5	25±5

Notes: $S_{E,P\_areal} = S_{E,P}$ reported in Table 11 = areal ejecta-induced settlement; $S_{E,P\_localized}$ = localized ejecta-induced settlement; A_T = total settlement assessment area; V_E = total volume of ejecta within A_T; A_E = total area of ejecta within A_T; The estimates of both areal and localized ejecta-induced settlement are rounded to the nearest 5; Final plus/minus values are also rounded to the nearest 5.

Table 14b: Areal and localized ejecta-induced settlement estimates for Patch A (20-m buffer) based on photographic evidence.

Earthquake Event	A_T (m^2)	A_E (m^2)	V_E (m^3)	S_{E,P_areal} (mm)	$S_{E,P\_localized}$ (mm)
Sep-10	1257	0	0	0	0
Feb-11	1257	1257	14.2-25.0	15±5	15±5
Jun-11	1257	907	13.9-24.6	15±5	20±5
Dec-11	1257	772	10.1-20.1	10±5	20±5

Notes: $S_{E,P\_areal} = S_{E,P}$ reported in Table 11 = areal ejecta-induced settlement; $S_{E,P\_localized}$ = localized ejecta-induced settlement; A_T = total settlement assessment area; V_E = total volume of ejecta within A_T; A_E = total area of ejecta within A_T; The estimates of both areal and localized ejecta-induced settlement are rounded to the nearest 5; Final plus/minus values are also rounded to the nearest 5.

Table 14c: Areal and localized ejecta-induced settlement estimates for Patch A (50-m buffer) based on photographic evidence.

Earthquake Event	A_T (m^2)	A_E (m^2)	V_E (m^3)	S_{E,P_areal} (mm)	$S_{E,P\_localized}$ (mm)
Sep-10	6170	0	0	0	0
Feb-11	6170	5634	73.7-130	15±5	20±5
Jun-11	6170	3807	61.7-108	15±5	25±5
Dec-11	6170	2774	30.4-60.7	10±5	15±5

Notes: $S_{E,P\_areal} = S_{E,P}$ reported in Table 11 = areal ejecta-induced settlement; $S_{E,P\_localized}$ = localized ejecta-induced settlement; A_T = total settlement assessment area; V_E = total volume of ejecta within A_T; A_E = total area of ejecta within A_T; The estimates of both areal and localized ejecta-induced settlement are rounded to the nearest 5; Final plus/minus values are also rounded to the nearest 5.

Summary 2:

The best estimate of the localized ejecta-induced free-field ground settlement at the Shirley Boys' High School site for the SEP 2011, FEB 2011, JUN 2011, and DEC 2011 earthquake is 0 mm, 15±5 mm, 20±5 mm, and 20±5 mm, respectively.